Geology, alteration and mineralization of the Ajax East and Ajax West copper-gold alkalic porphyry deposits, southern Iron Mask batholith, Kamloops, British Columbia

K.V. ROSS
Geological Survey of Canada, Vancouver, British Columbia

C.I. GODWIN
The University of British Columbia, Vancouver, British Columbia

L. BOND
Highland Valley Copper Mines, Logan Lake, British Columbia

K.M. DAWSON
Geological Survey of Canada, Vancouver, British Columbia

ABSTRACT

The Ajax East and Ajax West deposits are two of a number of porphyry Cu-Au deposits hosted by the alkaline Iron Mask batholith, in southern Quesnellia. The northwesterly trending batholith is an Early Jurassic composite intrusion emplaced in the Nicola Group, an intraoceanic island arc package.

Pit mapping delineated seven rock units: Nicola Group volcanic rocks, picrite, and five intrusive units ranging in composition from diorite or gabbro to quartz monzonite. The Ajax deposits occur at the contact between two phases of the Iron Mask pluton, the hybrid diorite and the younger Sugarloaf diorite, which is the probable source of copper-gold mineralization.

Porphyry-style mineralization consists of pyrite, chalcopyrite and minor molybdenite. Alteration has been divided into: (1) pre-main stage alteration, (2) main stage porphyry alteration, (3) late main stage alteration, and (4) post-porphyry alteration. Four main stage porphyry alteration assemblages have been defined: propylitic, albitic, potassic and scapolitic. Propylitic alteration, which occurs peripheral to albitic alteration, appears to be a weaker manifestation of the albitic assemblage. Albitic alteration is intensely developed along the contact of the Sugarloaf diorite and the hybrid diorite. Potassic and scapolitic vein assemblages cross-cut propylitic and albitic alteration assemblages. Pyrite and chalcopyrite are present in all main stage alteration assemblages but are most closely associated with albitic alteration. The Sugarloaf diorite is the most favourable host. Albitic alteration liberates Fe^{+} and may decrease pH, assisting in the precipitation of chalcopyrite. Alteration style is partially controlled by host lithology. Main stage alteration assemblage minerals overprint several deuteric alteration assemblages and are overprinted in turn by a low-grade regional metamorphic assemblage.

Remnants of hornfelsic Nicola Group volcanic rocks and serpentinized picrite are distributed along major fault systems that have also controlled the distribution of the younger phases of the batholith and are good indicators of potential zones of mineralization.

Introduction

The Ajax East and Ajax West deposits (Fig. 1) are two of a number of porphyry copper-gold deposits in the Afton mining district. The district is located southwest of Kamloops, 360 km northeast of Vancouver (Fig. 2), within the alkaline Iron Mask batholith. This northwesterly trending batholith is an Early Jurassic (207 ± 3 Ma, Mortensen et al., this volume) composite intrusion that occurs in the southern part of Quesnellia in the Intermontane Belt. The batholith is approximately 22 km long and 5 km wide. The Ajax deposits, near the southwestern edge of the batholith (Fig. 2, 50° 36′N, 120° 24′W), occur along the contact of two major dioritic phases of the Iron Mask pluton. These deposits have been classified with the silica-saturated group of alkalic porphyry deposits (Lang et al., 1992).

History

Exploration for copper within the Iron Mask batholith dates back to the late 1890s when exploration and development were carried out on a number of prospects including the original Pothook showing near Afton, and the showings which developed into the Ajax deposits. In 1896, the first year in which mining activity was recorded, over 200 claims were recorded on the batholith. By 1900, surface and underground work had been done on many of the properties. Most deposits, with the exception of the Iron Mask and Erin deposits, produced only a few tonnes of selective high-grade copper ore. The Iron Mask and Erin orebodies produced 165 557 tonnes of 1.47% Cu, 0.67 g/t Au and 2.67 g/t Ag during intermittent operation from 1904 to 1928. Other significant early prospects included the Python (Makaoo), Noonday, Lucky Strike, Iron Cap, Kimberly, and the Ajax, Wheal Tamar and Monte Carlo showings (Fig. 2).

Exploration on the Iron Mask batholith continued sporadically during the first half of the century. The Ajax, Wheal Tamar and Monte Carlo claims were among the early exploration targets on the Iron Mask batholith. By 1900, trenching and some underground work had been done on the Wheal Tamar claim, the site of the current Ajax East pit. Trenching was carried out on the Ajax claim between 1904 and 1910 and additional underground development and sampling was done in the next two decades. In 1916, Granby Mining and Smelting optioned and drilled several properties on the Iron Mask including the Wheal Tamar claim. In 1929, Consolidated Mining and Smelting Company trenched and sampled the area and drilled ten surface holes. Berens River Mines Limited (Newmont) optioned the property in 1952 and drilled a high-grade shear

FIGURE 1. View looking northwest over the Ajax East pit (right) and waste dump (left) in the foreground, the Ajax West pit in the centre and Jacko Lake in the background. (Photo taken October 1990.)

zone on the Monte Carlo claim. In 1954 Cominco optioned the four original Crown Grants and staked additional ground. Rolling Hills Copper Mines Ltd. conducted geological mapping and magnetic and induced polarization surveys in the early 1970s. The original Afton claims were staked in 1949 but the orebody was not discovered until 1970 when it was drilled by Afton Mines Limited. With that discovery, interest in the area was rekindled and mining and exploration activity have been ongoing since that time.

In 1980, Cominco, under a joint venture agreement with E & B Explorations Limited, initiated a major exploration program which continued through 1981. Work included 16 063 m of percussion drilling, 2465 m of diamond drilling and approximately 70 km of ground magnetometer and induced polarization surveys. With these expenditures E & B Explorations Limited acquired a thirty per cent interest in the property. Results of the program indicated a large *low-grade deposit with open pit potential.*

In 1986, an agreement was reached between Cominco, E & B Explorations and Afton Operating Corporation (the latter being a partnership between Teck Corporation and an affiliate of Metall Mining Corporation, until 1991 when Teck acquired full ownership of Afton Operating Corporation) under which Afton acquired a controlling interest in the Ajax property in respect to certain expenditures. During 1987, Afton carried out an extensive drilling and evaluation project leading to the decision to place the property into production. Thirty-one NQ diamond drill holes, totaling 3851 m, were drilled in the Ajax East deposit. Forty-six NQ diamond drill holes, totaling 7608 m, were drilled in the Ajax West deposit. Further percussion and diamond drilling was completed on the property as development advanced. By 1990, total drilling on the Ajax property, by all operators, included 21 428 m of percussion drilling and 29 782 m of diamond drilling.

Mining

A 10 km haulroad provides access to the Ajax deposits from the Afton milling complex. The haulroad passes under the Coquihalla Highway through an underpass installed during highway construction. It also passes over an existing secondary highway to Lac Le Jeune, utilizing a large steel culvert overpass installed as part of the Ajax project.

The deposits were developed in three stages. An initial higher grade pit was established on the northwest side of the West zone and first mined in June of 1989. Mining of this pit was completed in March of 1990. Development of the East zone pit began in November of 1989 and mining was in progress when operations were put on hold in August of 1991. A second stage pit was planned to release the remainder of the West zone reserves and pre-stripping was in progress on this phase at the time of shutdown. Total production from the Ajax deposits up to August of 1991 was 5.8 million tonnes at a grade of 0.50% Cu and 0.37g/t Au.

The mine reopened in September 1994 with reserves estimated at 14.1 million tonnes grading 0.46% Cu and 0.34 g/t Au. Ore is processed at the nearby Afton mill with a daily capacity of 8500 tonnes.

Mining equipment for the Ajax project was moved from the Afton area pits as operations there were wound down. The fleet

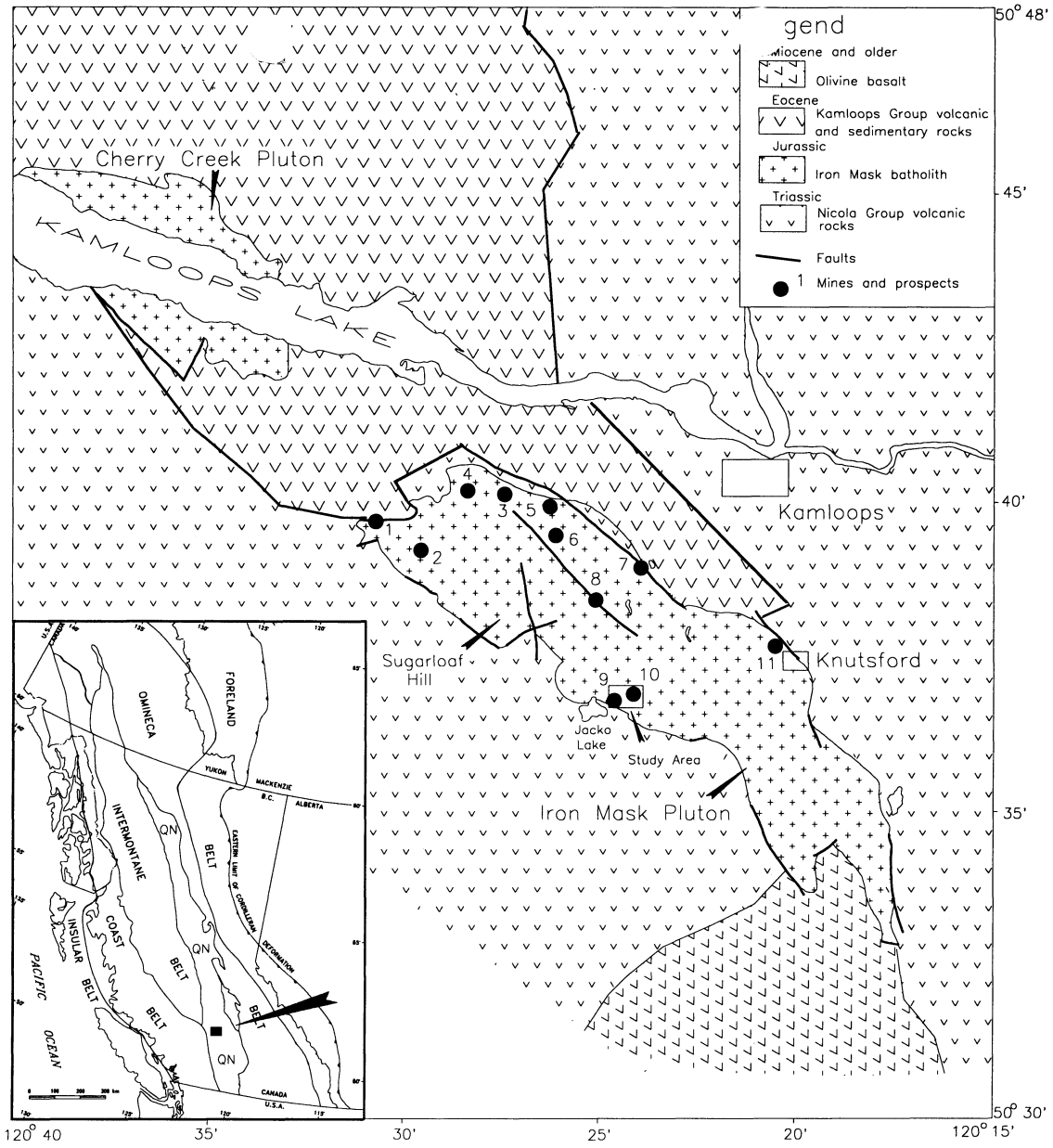

FIGURE 2. Regional geology of the Iron Mask and Cherry Creek plutons. Ajax East and Ajax West pits are located near the centre of the southwestern side of the Iron Mask batholith, immediately east of Jacko Lake. Deposits hosted within the Iron Mask pluton are: 1 = Afton; 2 = Pothook; 3 = Cresent; 4 = DM; 5 = Big Onion; 6 = Iron Mask and Erin; 7 = Python; 8 = Galaxy; 9 = Ajax West pit; 10 = Ajax East pit; and 11 = Kimberly. Terrane map inset locates the area within Quesnellia (QN) of the Intermontane Belt, Canadian Cordillera.

consisted of three P & H 1900 shovels, two Bucyrus-Erie 45R blasthole drills, one D40K Driltech, ten Unit Rig M-120 haul trucks, three Caterpillar D-8 tracked dozers, one Caterpillar 824B wheel dozer, two graders and three water trucks. Mining was done on 10 m benches with berms maintained on alternate benches. Overall pit slope angles varied depending on geotechnical constraints and ranged from 37 degrees to 51 degrees. Two blast patterns were utilized; a main production blast pattern, and a buffer blast pattern against final walls. Blastholes were loaded with Anfo or slurry if the holes were wet. Blasthole cuttings were sampled and analyzed for copper and gold. The Unit Rig M-120 haul trucks were used for both the ore haul and the waste or overburden removal. Ore from the Ajax pits was hauled over the 10 km haulroad to the Afton mill for processing. The round trip took approximately 1 hour for the M-120 haul trucks. The topography was favourable with an over-all grade of 2 per cent down to the mill. Consideration was being given to using a higher speed truck or truck-trailer combination for the ore haul at the time of shutdown.

Two main waste dumps and a low-grade stockpile were established at the Ajax site. Glacial till from pre-stripping was stockpiled for reclamation. Waste dumps were built in lifts with 20 m terraces or berms on which overburden was stockpiled to facilitate reclamation. As each lift was completed, the dump face was flattened to a reclaimed slope of 24 degrees to 28 degrees. Ditches and sedimentation ponds were constructed to collect runoff water from all disturbed areas before release to natural drainage systems. A clay-lined channel was constructed to carry Peterson Creek water from Jacko Lake through the mine site without the risk of contamination or loss. The main haulroad was treated with a $MgCl_2$ solution for dust control. A separate dry facility was established adjacent to the Ajax site to minimize travel time for mine crews. All other maintenance, crushing, and milling operations were carried out at the Afton site. The total workforce during the Ajax operation was approximately 200 personnel, with 75 working in mine operations.

Run-of-mine material was crushed to −8 inch at the Afton

TABLE 1. Whole rock analyses of major rock units

Units		90101 picrite	90102 picrite	KR92-28 Nicola Group volcanic rock	KR92-01 pegmatitic hybrid diorite	KR92-02 hybrid diorite	KR92-03 hybrid diorite	KR92-24 hybrid diorite	90108 hybrid diorite
SiO_2	%	43.2	44.7	48	41.4	51.5	51.9	41.6	46.8
TiO_2	%	0.296	0.518	0.555	0.741	0.886	0.744	0.977	0.823
Al_2O_3	%	5.77	7.58	11.8	19	16.1	18.6	7.03	17.8
Fe_2O_3	%	9.62	9.79	10.3	13.3	8.92	7.71	19.2	10.1
FeO	%	4	6.2	6.5	4.8	5	3.6	7.4	5
MnO	%	0.15	0.17	0.2	0.13	0.17	0.15	0.17	0.15
MgO	%	27.6	21.7	11.8	5.88	4.21	3.2	10.8	6.45
CaO	%	6.02	8.35	10.2	16	9.39	6.76	15.4	9.63
Na_2O	%	0.21	0.55	1.69	0.81	3.41	4.07	0.71	2.96
K_2O	%	0.96	0.65	1.47	0.29	1.95	2.6	0.99	1.79
P_2O_5	%	0.12	0.14	0.24	0.07	0.36	0.46	0.12	0.33
H_2O^+	%	5.3	4.1	2.2	1.4	1.6	1.8	1.4	2.5
H_2O^-	%	0.2	0.3	0.1	0.2	0.2	0.2	0.2	0.2
CO_2	%	0.1	0.07	0.11	0.51	0.13	0.2	0.22	0.59
LOI	%	5.45	4.15	1.7	1.35	1.95	1.7	1.5	3.25
SUM	%	99.80	98.61	98.21	99.70	98.80	98.80	98.56	100.32
Au	ppb	−5	−5	7	−5	−5	−5	−5	12
S	ppm	−50	−50	−50	−50	399	2320	−50	1020
F	ppm	280	168	249	56	350	500	439	388
Na	ppm	1700	4400	13000	7900	24000	30000	5900	23000
Cl	ppm	196	221	484	262	385	412	696	433
Sc	ppm	22.2	30.3	31.4	41.8	23.8	11.1	109	26.6
V	ppm	131	145	279	323	259	285	303	353
Cr	ppm	2250	1820	700	39	73	33	139	207
Co	ppm	86	73	49	35	23	16	59	38
Ni	ppm	1060	817	273	76	19	7	58	64
Cu	ppm	30	22	184	4	53	45	39	379
Zn	ppm	47	61	70	67	61	47	69	56
As	ppm	5	2	3	−2	−2	2	3	2
Br	ppm	2	2	1	3	3	2	3	1
Rb	ppm	38	18	55	−20	−20	40	18	42
Sr	ppm	61	55	464	731	857	901	150	743
Y	ppm	−2	−2	−2	−10	15	10	−2	−2
Zr	ppm	13	45	29	−10	82	40	17	23
Nb	ppm	5	5	5	2	6	9	5	6
Sb	ppm	0.4	0.2	0.2	0.2	0.2	0.3	0.3	3.7
Cs	ppm	1	−1	−1	1	1	1	2	−1
Ba	ppm	561	259	780	102	787	1720	141	919
La	ppm	2.1	3.1	9.8	1.3	9.7	8.7	2.5	7
Ce	ppm	6	9	19	4	22	20	7	17
Nd	ppm	−5	5	8	−5	12	12	−5	10
Sm	ppm	0.8	1.4	1.7	1	2.8	2.9	1.5	2.6
Eu	ppm	0.2	0.7	0.5	0.5	0.8	0.6	0.9	0.7
Yb	ppm	0.6	1.1	1	0.6	1.9	1.9	0.6	1.8
Lu	ppm	0.15	0.16	0.17	0.08	0.27	0.28	0.13	0.25
Hf	ppm	−0.5	1.1	0.9	−0.5	1.7	1.7	0.8	1
Th	ppm	−0.5	−0.5	0.8	−0.5	1.3	1.1	−0.5	−0.5
U	ppm	−0.5	−0.5	−0.5	−0.5	0.9	0.6	−0.5	−0.5

crusher and stockpiled. To increase throughput of the fine-grained, albitized Ajax ore, the original Afton SAG mill-ball mill grinding circuit was converted to a SAG mill-ball mill-crusher configuration. This involved installation of large pebble ports in the SAG mill to release coarser material, and the addition of a pebble crusher to the circuit to reduce some of the coarse SAG mill product from 2½ inches to ⅜ inch. Discharge from the grinding circuit was sent to a flotation circuit consisting of roughing, scavenging, regrinding and multiple cleaning stages. Mill throughput averaged 9000 tonnes per day prior to shutdown. Recoveries were approximately 80% for both copper and gold.

Exploration Techniques

The Ajax deposits were first noted in surface outcrop and early exploration consisted of prospecting, trenching and some underground development. Extensive percussion and diamond drilling outlined the deposits and built up reserves. Later operators conducted geochemical and geophysical surveys over the property. A magnetic survey over the ore zone returned a weak response as magnetite is largely destroyed by albitization. The soil anomaly is restricted to the immediate area surrounding the outcrop area due to thick buildups of glacial till adjacent to the deposits. An induced polarization survey obtained an anomalous response in stronger pyrite mineralization peripheral to the copper-gold deposits.

Regional Geology

The Iron Mask batholith intruded Carnian to Norian Nicola Group volcanic rocks (Preto, 1977) of the Quesnellia intraoceanic island arc terrane (Souther, 1992). Contemporaneous calc-alkaline and alkaline batholiths emplaced in the Quesnellia terrane are host to numerous porphyry copper deposits. Calc-alkaline volcanic rocks occur in the west, grading to increasingly more alkaline rocks to the east, possibly reflecting an east dipping subduction zone (Monger et al., 1991). Major plutonic events (Preto et al., 1979) occurred at about 200 Ma, 160 Ma, 100 Ma and 50 Ma to 70 Ma. The 200 Ma group includes plutons of both the alkaline, i.e., Copper Mountain, and calc-alkaline series. The younger events comprise only calc-alkaline, i.e., Guichon plutonic suites (Woodsworth et al., 1992).

The Iron Mask batholith is one of the larger alkaline intrusions of the 200 Ma group and consists of the Iron Mask and the Cherry Creek plutons. A recent revision of the geology of the Iron Mask batholith is presented by Snyder and Russell (1993; this volume) and Stanley et al. (1994). Significant changes to the earlier interpretations of Preto (1967) and Northcote (1974, 1976, 1977) are the designation of the Iron Mask hybrid diorite as a facies of the Pothook diorite, and the determination that the picrite is genetically unrelated to the batholith. The Iron Mask pluton consists of three major phases: the Pothook diorite, the Cherry Creek diorite and the Sugarloaf diorite. An easterly trending graben filled with

TABLE 1. (continued)

Units		DY3474 Sugarloaf diorite	KR92- Sugarloaf microdiorite	KR92-26 Sugarloaf diorite	KR92-27 monzodiorite dike	KR92-64 monzodiorite dike	-107 monzodiorite dike	KR92-06 monzodiorite dike	DY3463 quartz eye latite dike
SiO_2	%	54.6	49.4	54.9	58.2	55.6	55.4	50	51.1
TiO_2	%	0.67	0.825	0.647	0.484	0.556	0.562	0.602	1.2
Al_2O_3	%	18	15.1	18.2	18.4	18.5	17.7	17.5	14.7
Fe_2O_3	%	7.03	9.92	6.83	5.31	2.4	6.91	8.73	6.86
FeO	%	3	5.9	3.8	1.3	1.1	2.8	4	4.4
MnO	%	0.08	0.14	0.11	0.04	0.07	0.04	0.05	0.11
MgO	%	3.21	8.15	3.22	1.63	3.09	2.54	3.13	6.81
CaO	%	7.31	9.13	7.33	5.3	9.57	5.27	5.05	7
Na_2O	%	5.95	2.58	5.63	5.89	6.8	4.58	5.01	4.13
K_2O	%	1.2	1.72	1.56	2.14	0.45	4.23	3.31	1.88
P_2O_5	%	0.24	0.24	0.25	0.23	0.29	0.27	0.36	0.4
H_2O^+	%	1.3	2.1	1.1	1.4	1.9	1.4	2	2.4
H_2O^-	%	0.1	0.2	0.1	0.3	0.2	0.1	0.2	0.2
CO_2	%	0.69	0.16	0.09	0.08	1.06	1.04	2.6	1.69
LOI	%	2.05	1.95	1.15	2	3.05	2.6	5.3	4.05
SUM	%	100.50	99.41	99.98	99.88	100.48	100.46	98.50	98.41
Au	ppb	10	7	−5	41	−5	24	−5	10
S	ppm	−50	98	−50	−50	−50	−50	−50	−50
F	ppm	304	287	256	198	240	312	290	640
Na	ppm	42000	21000	42000	44000	50000	35000	35000	30000
Cl	ppm	377	568	586	208	161	374	245	173
Sc	ppm	16.6	34.5	17.3	7.5	13.5	13.4	14.3	18.4
V	ppm	234	263	234	129	121	209	197	180
Cr	ppm	86	363	66	67	49	63	13	265
Co	ppm	18	39	22	13	11	18	17	32
Ni	ppm	12	140	11	10	3	11	12	150
Cu	ppm	50	151	51	263	68	340	2	28
Zn	ppm	42	47	38	32	23	36	35	58
As	ppm	7	2	−2	6	2	6	−2	12
Br	ppm	2	2	3	3	2	4	2	4
Rb	ppm	35	54	43	31	14	50	40	45
Sr	ppm	610	506	631	795	509	586	486	497
Y	ppm	−2	3	7	3	−2	−2	−10	−2
Zr	ppm	84	70	71	72	67	72	55	155
Nb	ppm	5	6	6	10	6	5	8	23
Sb	ppm	0.2	0.4	−0.2	0.3	0.2	10	0.2	0.5
Cs	ppm	−1	−1	1	1	−1	1	1	2
Ba	ppm	441	1090	472	1190	166	2350	1830	345
La	ppm	8.7	7.7	7.3	10.4	10.2	11.5	10.5	23.5
Ce	ppm	21	18	17	24	24	25	22	50
Nd	ppm	10	10	11	12	13	12	11	23
Sm	ppm	2.5	2.6	2.6	2.7	2.9	2.7	2.2	4.5
Eu	ppm	1.2	0.9	0.9	0.8	1.1	1.2	0.8	1.4
Yb	ppm	1.9	2	2	1.8	1.7	1.8	1.3	1.4
Lu	ppm	0.3	0.3	0.31	0.32	0.28	0.32	0.22	0.25
Hf	ppm	2.1	1.6	2.1	2	2	2	1.3	3.6
Th	ppm	1.5	1	1.2	1.5	1.6	2.1	1.7	3.2
U	ppm	1.3	1	1	1.9	1.8	2.5	1.3	1.2

up to 1000 m of Middle Eocene Kamloops Group volcanic and sedimentary rocks separates the plutons at surface.

Property Lithology, Petrography and Geochemistry

Geologic maps and cross-sections of the two pits are presented in Figures 3 and 4. The major lithologies can be divided into premineral, synmineral and postmineral groups. The chemistry of least-altered rocks are presented in Table 1 and plotted in Figures 5 and 6. The intrusions lie near the alkaline/subalkaline boundary (Fig. 5). In a K_2O vs Na_2O plot (Fig. 6) of the the alkalic suite, the samples lie in both the sodic and potassic fields.

Premineral Lithologies

Nicola Group volcanic rocks (unit 1) are sub-alkaline basalts which host the Iron Mask batholith and are in part, coeval with it (Preto, 1977). They crop out 500 m south of the Ajax West pit along the margins of Jacko Lake (Fig. 2). Two large unmineralized, relatively unaltered remnants of Nicola Group volcanic rocks occur within the Sugarloaf diorite in the Ajax West pit (Fig. 3). A 5 m wide hornfelsic remnant of Nicola Group volcanic rocks, striking 040°, occurs along the contact between the two main dioritic units (Sugarloaf and hybrid diorites) in the Ajax East pit (Fig. 4). Outside the pits, the Nicola Group volcanic rocks are dark green to black, medium-grained, augite phyric and non- to weakly magnetic. In thin section euhedral augite phenocrysts are pseudomorphed by blue-green to yellow hornblende and occur in a trachytic matrix of cloudy feldspar laths and fine-grained hornblende. Secondary red-brown biotite is also weakly developed in the matrix. In the foliated volcanic rocks in the Ajax East pit, the augite phenocrysts are totally replaced by pale green amphibole in a groundmass of medium-grained red-brown biotite and fine-grained hornblende and sericite. Numerous dikes and dikelets of Sugarloaf diorite intrude the screen.

Picrite (unit 2) occurs predominantly south of the Ajax West pit, where holes drilled in 1990 intersected as much as 150 m of serpentinized picrite. Lenses of picrite are also found along the major faults that separate the two main dioritic units (hybrid and Sugarloaf diorites). The picrite also occurs outside the batholith (Cockfield, 1948; Carr, 1956; Snyder and Russell, 1993) and has no genetic relationship to batholithic rocks (Snyder and Russell, 1993).

The picrite is a dark grey rock in which an aphanitic matrix surrounds rounded, darker phenocrysts of olivine or rarely pyroxene that are partially to completely replaced by serpentine and magnetite. On sheared surfaces, waxy serpentinite is characteristic. The picrite is strongly magnetic. In thin section, the corroded, serpentinized, coarse-grained olivine and relict clinopyroxene

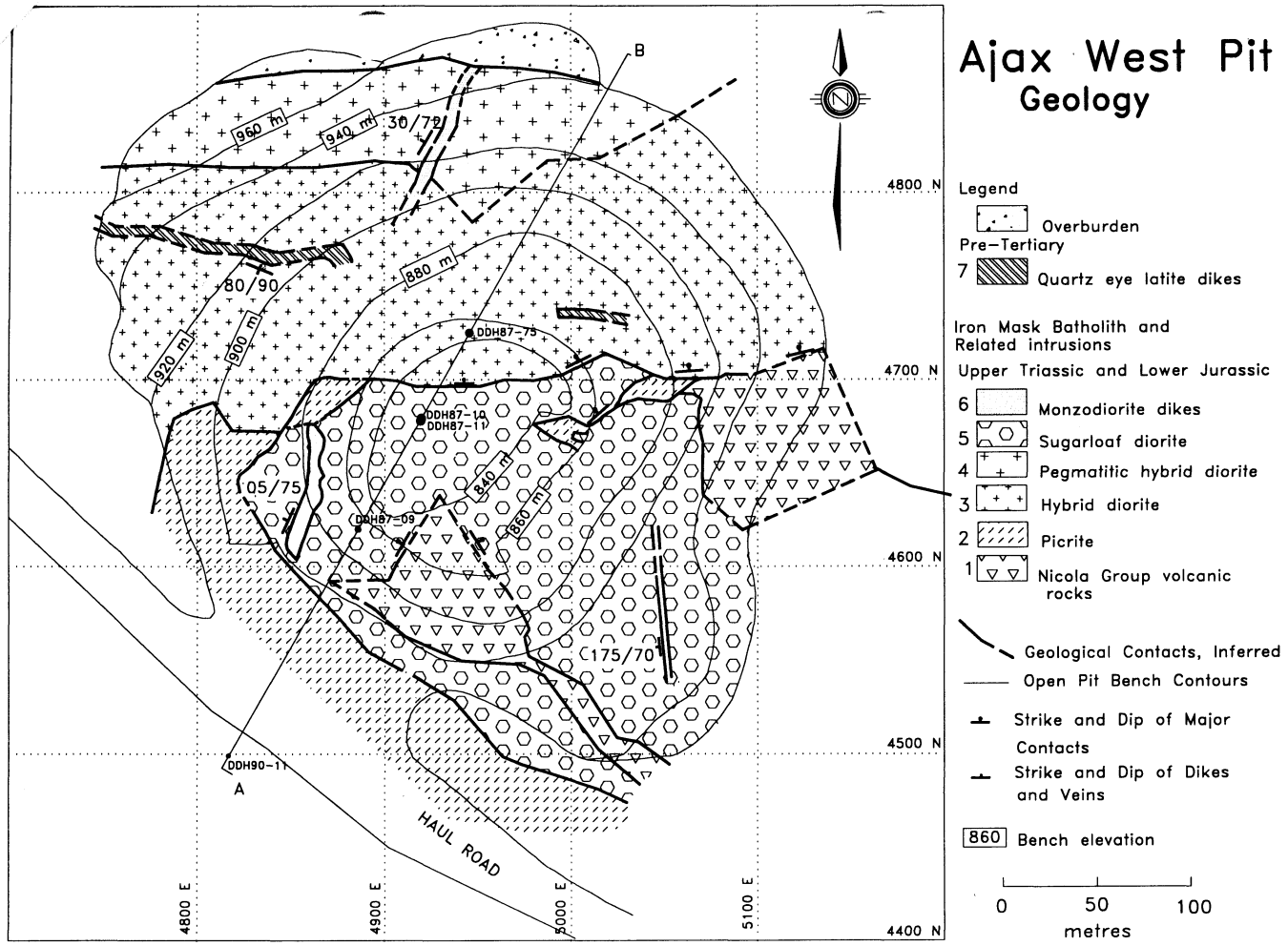

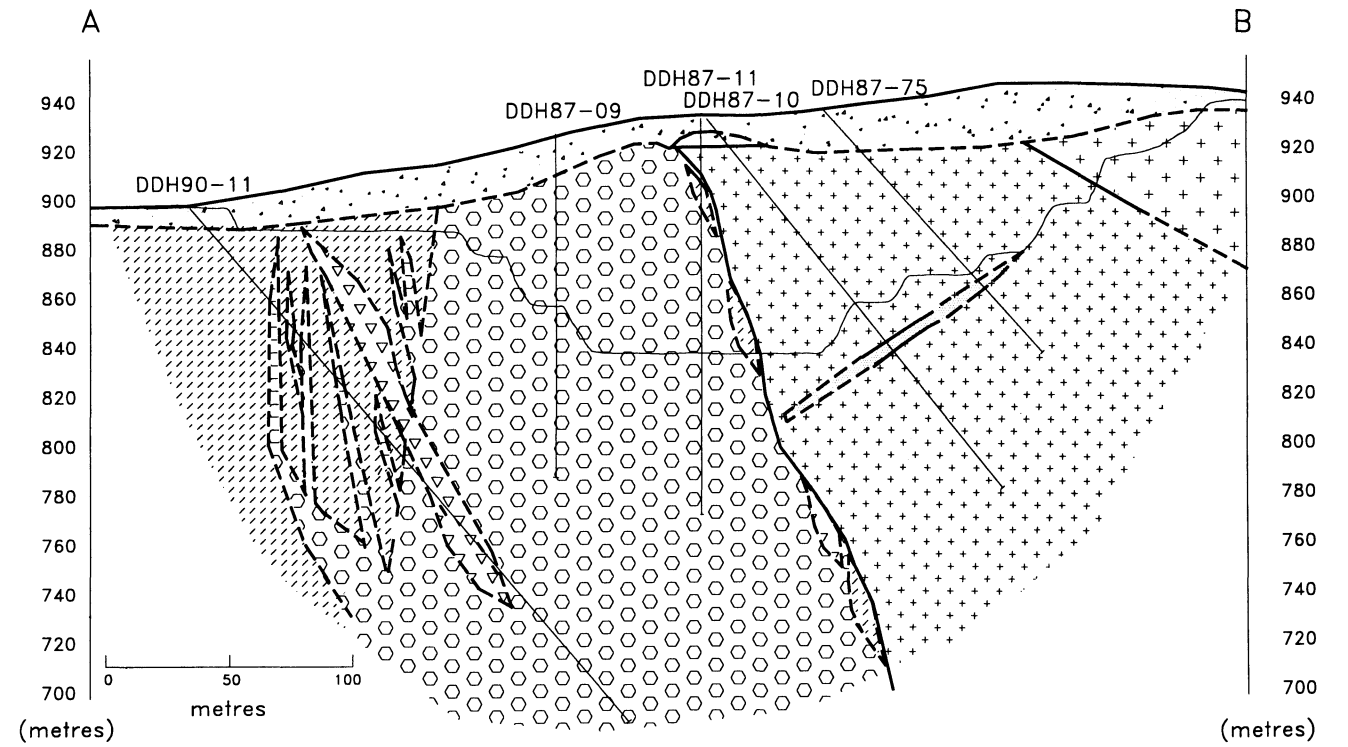

Ajax West Pit, Cross Section 12.5 W

FIGURE 3. Geological map and cross-section of the Ajax West pit.

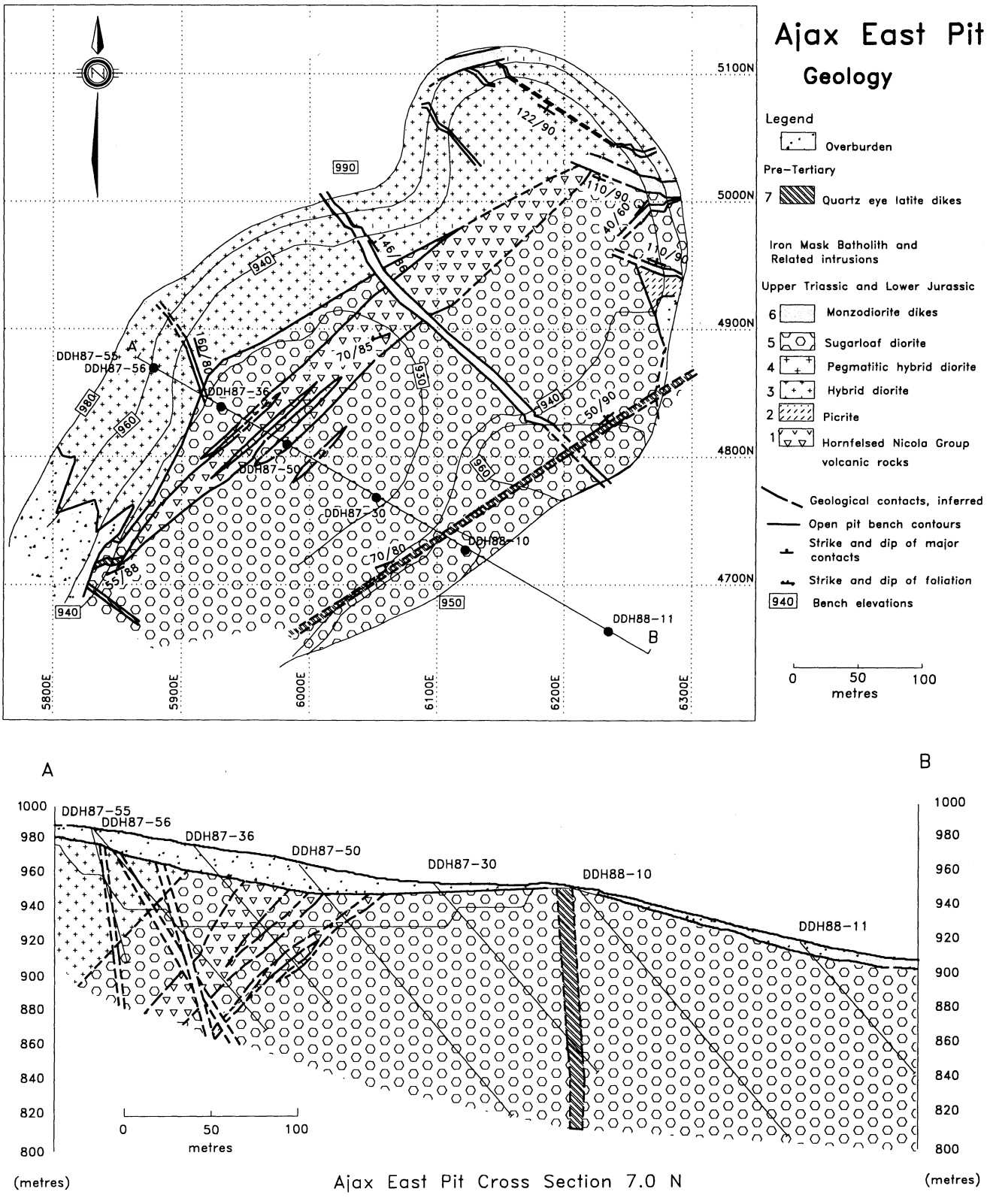

FIGURE 4. Geological map and cross-section of the Ajax East pit.

phenocrysts are set in a groundmass of aphanitic to fine-grained, grey serpentine with needles of tremolite. The picrite is cut by dikes of trachytic Sugarloaf diorite.

Hybrid diorite (unit 3) is a medium grey to green rock, that ranges from a fine-grained diorite to a coarse-grained pyroxenite (Fig. 7 A,B,C). Recent work (Snyder and Russell, 1993) indicates the hybrid diorite is a phase of the Pothook diorite that has assimilated variable amounts of Nicola Group volcanic rocks. However, hybrid diorite near the Ajax pits has only local development of poikiolitic biotite and lacks the magnetite veinlets and schlieren characteristic of Pothook diorite (Stanley et al., 1994). Therefore, for clarity and continuity with previous literature (Kwong, 1987; Ross et al., 1992, 1993), the term hybrid diorite will be retained in this paper. A coarse-grained, hornblende-rich unit has been mapped separately as pegmatitic hybrid diorite, (unit 4). All phases are strongly magnetic. In the Ajax West pit, the fine-grained dio-

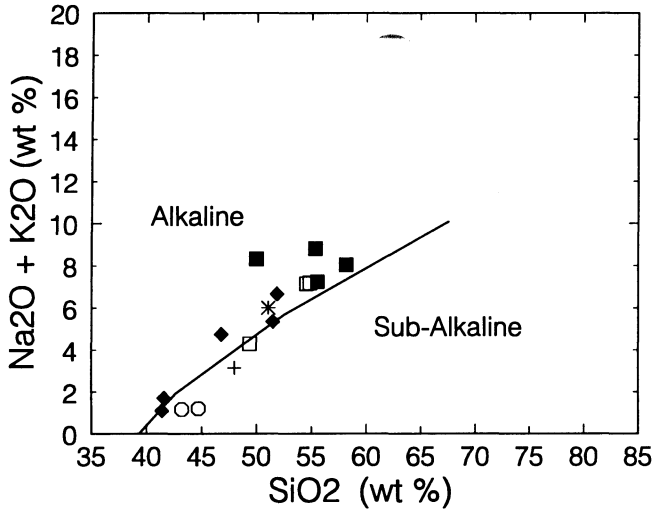

+ Nicola Group volcanic rock
○ picrite
◆ hybrid diorite
□ Sugarloaf diorite
■ monzodiorite dike
✳ quartz eye latite dike

FIGURE 5. Classification of rocks from the Ajax East and Ajax West pits on an alkaline affinity diagram (Irvine and Baragar, 1971). Symbols are defined in the legend.

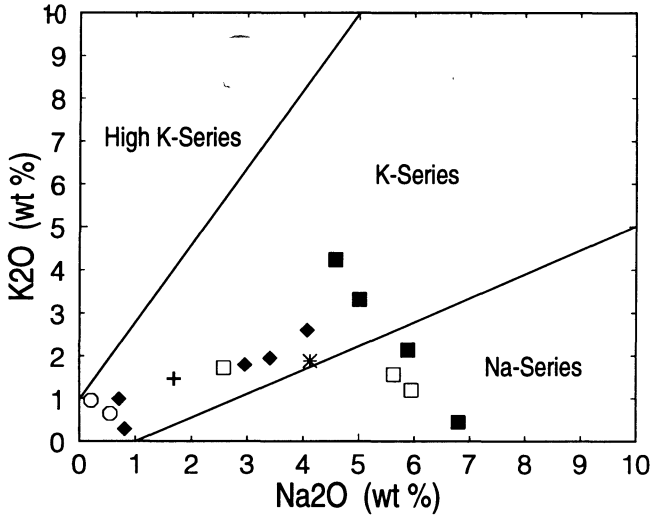

FIGURE 6. Classification of rocks from the Ajax East and Ajax West pits on a Na_2O/K_2O discrimination diagram, (after Middlemost, 1975). (See legend in Fig. 5.)

ritic phase predominates to the north of a major fault that trends eastward and separates the hybrid diorite from the Sugarloaf diorite. The fine-grained texture may be the result of chilling of the magma along the batholith margin. In the Ajax East pit (Fig. 4) a dark grey-green, medium- to coarse-grained, pyroxene-rich phase occurs on the northwestern side of the pit, separated from the Sugarloaf diorite by a fault and hornfelsic Nicola Group volcanic rocks.

In thin section the fine-grained diorite consists of pale green pyroxene, plagioclase, pale green hornblende, red-brown biotite and magnetite. Textural varieties include those characterized by: (1) twinned plagioclase grains, smaller anhedral pyroxene grains and interstitial hornblende, magnetite and biotite, (2) equigranular, interlocking pyroxene and weakly twinned plagioclase with interstitial biotite and magnetite, and (3) subhedral pyroxene and laths of plagioclase enclosed in poikiolitic red-brown biotite and poikiolitic plagioclase. The hybrid diorite in the Ajax East pit is characterized by two dominant types: (1) a medium- to coarse-grained phase with interlocking pyroxene grains and interstitial plagioclase and magnetite, and (2) a medium-grained phase with equant pyroxene phenocrysts in a groundmass of hornblende and plagioclase. The plagioclase is unzoned and ranges from andesine to labradorite (An_{41} to An_{57}). The pyroxene is diopside/salite.

Pegmatitic hybrid diorite (unit 4) is an agmatitic mixture of fine-grained to pegmatitic diorites and hornblendites. This unit occurs in the East pit as localized pockets. The unit outcrops in the upper benches of the Ajax West pit (Fig. 3), and occurs immediately north of the Ajax West and Ajax East pits. The coarsest material is dominated by hornblende laths up to 5 cm long with interstitial plagioclase and magnetite. Pyroxene, the most abundant mineral in the finer grained phases, is accompanied by twinned plagioclase, primary pale olive-green hornblende, a primary red-brown biotite and abundant interstitial coarse-grained magnetite. Secondary red-brown biotite is a common alteration of the hornblende.

Synmineral Lithologies

Sugarloaf diorite (unit 5) is a fine- to medium-grained porphyry that occurs as a lobe-shaped body along the margin of the hybrid diorite. In the Ajax West pit the unit occurs to the south of the major east-west fault. It occurs on the southeastern side of the Ajax East pit. Rock textures range widely from fine-grained and weakly porphyritic to a medium-grained, commonly trachytic porphyry (Figs. 7 D, 8 A). Over-all, Sugarloaf diorite is characterized by elongate hornblende and plagioclase phenocrysts enclosed in a grey matrix. Two fine-grained to aphanitic phases recognized in drill core were not distinguished in the pit mapping. An aphanitic, grey, weakly magnetic phase occurs as small (<0.5 metre) dikelets cross-cutting the more typical Sugarloaf diorite. Similar dikelets with disseminated chalcopyrite were observed 600 m east of the Ajax East pit. The second variety consists of equant, black phenocrysts (originally pyroxene?) in varying amounts in an aphanitic matrix. Uncertain and gradational contact relationships support contamination by assimilation of inclusions of Nicola Group volcanic rocks.

In thin section the typical porphyritic Sugarloaf diorite contains olive-green, strongly pleochroic, prismatic crystals, tabular laths and needles of hornblende. Tabular plagioclase feldspar phenocrysts are commonly sericitized. In several samples, large (5 mm long) phenocrysts exhibit oscillatory zoning, ranging from andesine (An_{30}) in the core to labradorite (An_{53}) on the rims. The groundmass is mainly aphanitic to microcrystalline, saussuritized plagioclase. Accessory minerals are subhedral, corroded apatite and microcrystalline magnetite. Common secondary minerals include blue-green hornblende and yellow-green epidote after primary hornblende. Quartz was observed in the groundmass of one sample.

Monzodiorite (unit 6) occurs as a prominent set of steeply dipping dikes trending northwest in both the Ajax West and Ajax East pits and cuts hornfelsic Nicola Group volcanic rocks, the hybrid diorite and the Sugarloaf diorite. The monzodiorite is a fine-grained, blue-grey to pinkish, amphibole and plagioclase phyric rock, commonly with pervasive yellow-green epidote alteration. The pinkish colour is due to pervasive K-feldspar alteration that occurs sporadically in some dikes but is absent in others. In thin section the monzodiorite (Fig. 8 B) is porphyritic with phenocrysts of tabular to equant well twinned plagioclase, prismatic pale green amphibole and minor pyroxene, in a feldspar groundmass. Common accessory minerals are subhedral apatite and magnetite in a matrix of aphanitic plagioclase. This unit was previously grouped with the Cherry Creek suite, but petrographic and geochemical data (Table 1) suggest a closer affiliation with the Sugarloaf diorite suite.

Postmineral Lithologies

Quartz eye latite dikes (unit 7) occur in both pits. In the Ajax West pit a single large dike can be traced across the northern half of the pit, where it cross-cuts the hybrid diorite (Fig. 3). It is disrupted by intense faulting in the northeast quadrant of the pit. In

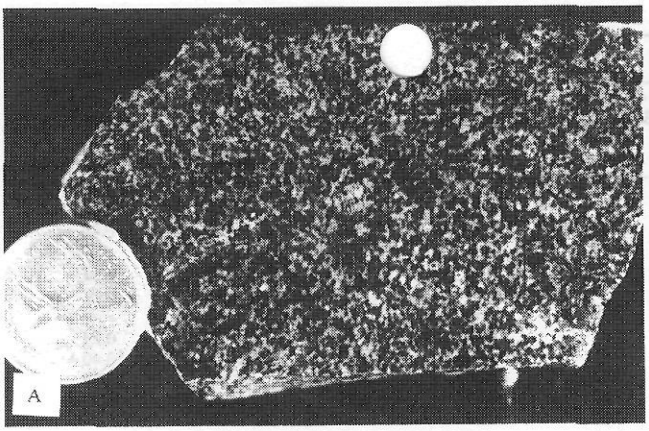

FIGURE 7A. Hand sample of medium-grained hybrid diorite. This unit displays considerable textural variation, ranging from a fine-grained dark grey unit to a pegmatitic unit, however mineralogy changes little. The mafic minerals are dominantly pyroxene, with minor poikiolitic biotite and primary amphibole. Magnetite is a common constituent, with up to 15% present in the coarser grained phases. The light coloured mineral is plagioclase. K-feldspar occurs locally.

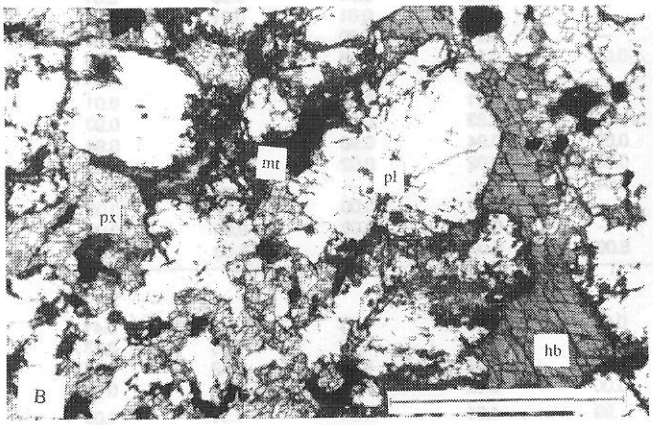

FIGURE 7B. Thin section of coarse-grained hybrid diorite exhibiting coarse-grained pyroxene and plagioclase with interstial magnetite and amphibole. Abbreviations: px = pyroxene, mt = magnetite, pl = plagioclase, hb = hornblende. (Scale bar 1 mm.)

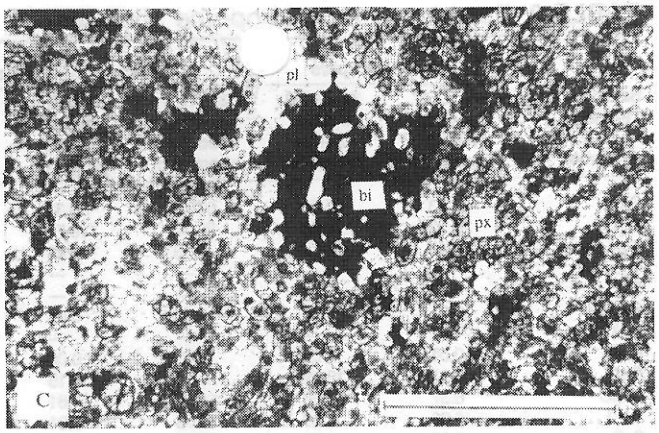

FIGURE 7C. Thin section of fine-grained hybrid diorite with a higher proportion of plagioclase, less magnetite and poikoilitic brown biotite enclosing pyroxene and plagioclase. Abbreviations: bi = biotite px = pyroxene, pl = plagioclase. (Scale bar 1 mm)

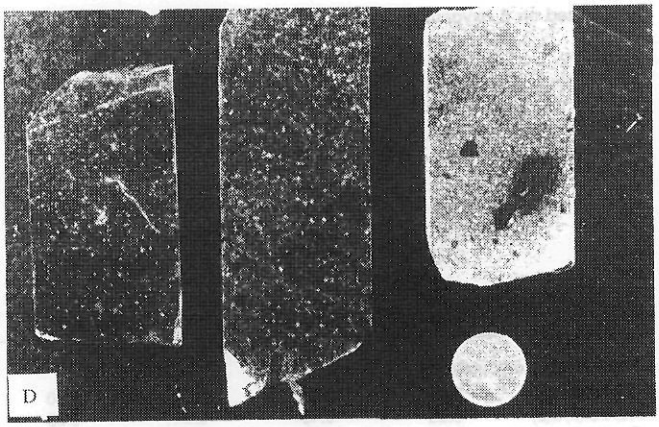

FIGURE 7D. Hand samples of Sugarloaf diorite exhibiting the range of textures. The first sample is medium grained, dominantly plagioclase-phyric with minor, finer-grained hornblende laths in a plagioclase matrix. The mafic clast is a common characteristic of the Sugarloaf diorite. The second sample is a medium-grained plagioclase-hornblende phyric phase. The third sample is a fine-grained phase with fewer plagioclase and hornblende laths set in an aphanitic plagioclase matrix.

the Ajax East pit (Fig. 4), two major dikes cut the Sugarloaf diorite and the picrite. The largest dike is approximately 5 m wide and is exposed over the entire length of the southeastern side of the pit. The second dike occurs at the contact between hybrid diorite and Sugarloaf diorite in the southwest corner of the pit. Several parallel dikelets were noted. These dikes post-date alteration, mineralization and many of the faults. Kwong (1987) concluded that similar-looking dikes in the Afton pit were pre-Tertiary.

This rock in hand sample is a uniform, fine-grained, porphyritic, brownish pink rock with hornblende needles and characteristic quartz and K-feldspar phenocrysts up to 1 cm long, some aggregates of coarse-grained K-feldspar and minor disseminated pyrite. Epithermal-style, vuggy quartz veins, accompanied by bleaching and silicification of the host rock, are associated with these dikes. In thin section fresh quartz eye latite is a mass of golden brown hornblende needles in a groundmass of K-feldspar and twinned plagioclase. The K-feldspar laths commonly have calcite in their cores. Chlorite with anomalous blue birefringence is common and unique to this unit.

Alteration and Mineralization

Alteration has been divided into four stages: (1) pre-main stage porphyry alteration, (2) main stage porphyry alteration, (3) late stage porphyry alteration and (4) post-porphyry alteration. The main stage alteration has been subdivided into four assemblages: propylitic, albitic, potassic, and scapolitic.

Premain Stage Alteration

Several types of alteration predate the main stage alteration and mineralizing event. The earliest alteration, serpentinization and hornfels, is related to the intrusion of the early phases of the batholith into picrite and Nicola Group volcanic rocks. Two types of deuteric alteration were observed, hornblende in the hybrid diorite and epidote in the pegmatitic hybrid diorite.

Serpentinization of picrite within the batholith is ubiquitous, whereas outside the batholith, picrite is relatively unaltered (Snyder and Russell, 1993). Picrite adjacent to and within the diorite units is pervasively altered to a fine-grained serpentinite with tremolite, magnetite and local relict olivine phenocrysts. Where picrite is intruded by mineralized Sugarloaf diorite, sulphide mineralization penetrates only a few centimetres. Picrite in the major fault on the eastern wall of the Ajax West pit has been altered locally to carbonate-quartz-fuchsite. This alteration is related to intense carbonate alteration of all units in the northeastern quadrant of the Ajax West pit.

The remnant of Nicola Group volcanic rocks that occurs along

TABLE 2. Representative microprobe analyses

	Primary feldspars		Secondary feldspars			Primary pyroxenes		Secondary pyroxenes	
Sample	33 A2 1	34 B11 2	31 A1 1	35 B10 3	42 B8 4	24 A1 5	35 B12 1	17 A4 7	45 A4 2
Lithology	Sugarloaf diorite	hybrid diorite	Sugarloaf diorite	hybrid diorite	Sugarloaf diorite	c.g. hybrid diorite	f.g. hybrid diorite	Sugarloaf diorite	hybrid diorite
Alteration	propylitic	propylitic	propylitic	propylitic	albitic	none	propylitic	albitic	albitic
SiO_2	57.33	54.39	67.49	68.34	68.02	52.94	53.81	54.15	54.22
Al_2O_3	26.93	28.88	20.20	19.74	20.05	1.24	0.33	0.34	0.46
K_2O	0.48	0.17	0.19	0.03	0.13	—	—	—	—
TiO_2	—	—	—	—	—	0.22	0.03	0.00	0.08
FeO	—	—	—	—	—	5.77	5.01	3.93	4.27
Fe_2O_3	0.21	0.25	0.03	0.08	0.00	—	—	—	—
MnO	—	—	—	—	—	0.22	0.21	0.13	0.24
MgO	0.01	0.00	0.03	0.00	0.01	14.98	15.23	15.85	16.40
CaO	8.62	10.99	0.79	0.15	0.35	23.64	24.57	24.66	23.78
Na_2O	6.37	5.15	11.02	11.61	11.35	0.31	0.21	0.24	0.30
BaO	0.03	0.00	0.03	0.01	0.00	—	—	—	—
SrO	0.07	0.08	0.00	0.00	0.00	—	—	—	—
Cr_2O_3	—	—	—	—	—	0.00	0.00	0.00	0.01
NiO	—	—	—	—	—	0.02	0.00	0.02	0.00
TOTAL	100.05	99.91	99.78	99.96	99.91	99.34	99.40	99.32	99.76
FeO/MgO	—	—	—	—	—	0.39	0.33	0.25	0.26
Ions based on 8 oxygens						**Ions based on 13 oxygens**			
Si	2.57	2.46	2.96	2.99	2.97	1.97	2.00	2.00	1.99
Al(IV)	1.42	1.54	1.04	1.02	1.03	0.03	0.01	0.00	0.01
Al(VI)	—	—	—	—	—	0.02	0.01	0.01	0.01
Ti	—	—	—	—	—	0.01	0.00	0.00	0.00
Fe^{+2}	0.01	0.01	0.00	0.00	0.00	0.18	0.16	0.12	0.13
Fe^{+3}	—	—	—	—	—	—	—	—	—
Mn	—	—	—	—	—	0.01	0.01	0.00	0.01
Mg	0.00	0.00	0.00	0.00	0.00	0.83	0.84	0.87	0.90
Ca	0.42	0.53	0.04	0.01	0.02	0.94	0.98	0.98	0.94
Na	0.55	0.45	0.94	0.98	0.96	0.02	0.02	0.02	0.02
K	0.03	0.01	0.01	0.00	0.01	—	—	—	—
Cr	—	—	—	—	—	0.00	0.00	0.00	0.00
Ni	—	—	—	—	—	0.00	0.00	0.00	0.00
(OH,O)	8.00	8.00	8.00	8.00	8.00	6.00	6.00	6.00	6.00
End member calculations									
KAlSi(3)O(8)	0.03	0.01	0.01	0.00	0.01	0.42	0.43	0.44	0.41
NaAlSi(3)O(8)	0.55	0.45	0.94	0.98	0.96	0.08	0.07	0.06	0.13
CaAl(2)Si(2)O(8)	0.42	0.53	0.04	0.01	0.02	0.49	0.49	0.49	0.45
(Mg Fe Sr)	0.01	0.01	0.00	0.00	0.00	0.02	0.02	0.02	0.04
TOTAL	1.01	1.00	.99	.99	.99	1.01	1.01	1.01	1.03

	Chlorite			Scapolite	Zeolite	Prehnite		Pumpellyite
Sample	43 A6 7	45 A3 1	49 B6 3	49 B2 1	49 B2 5	33 A10 3	38 B5 5	57 B8 8
Lithology	Sugarloaf diorite	Sugarloaf diorite	Sugarloaf diorite	hybrid diorite	hybrid diorite	Sugarloaf diorite	hybrid diorite	Sugarloaf diorite
Alteration	propylitic	potassic	albitic	scapolite	scapolite	propylitic	propylitic	albitic
SiO_2	27.30	28.79	29.37	55.67	62.63	43.97	42.43	37.47
Al_2O_3	17.88	17.92	17.17	23.12	15.16	23.87	23.12	26.65
K_2O	—	—	—	1.00	1.29	—	—	—
TiO_2	0.00	0.00	0.01	—	—	0.02	0.12	0.00
FeO	22.57	16.53	16.61	—	—	0.62	1.80	—
Fe_2O_3	—	—	—	0.12	0.02	—	—	6.75
MnO	0.22	0.24	0.07	—	—	0.08	0.05	0.05
MgO	17.51	22.34	22.99	0.00	1.75	0.01	0.26	0.79
CaO	0.02	0.01	0.03	6.43	4.05	26.79	26.48	22.95
Na_2O	0.05	0.02	0.05	10.06	0.27	0.02	0.01	0.01
Cl	—	—	—	3.59	14.82	—	—	—
TOTAL	85.55	85.85	86.30	99.99	99.99	95.38	94.27	94.67
FeO/MgO	1.29	0.74	0.72					
Ions based on 18 oxygens								
Si	5.47	5.64	5.77	7.59	21.52	6.03	6.52	6.49
Al	4.22	4.14	3.98	3.71	6.65	3.86	4.18	5.44
Ti	0.00	0.00	0.00	—	—	0.00	0.01	0.00
Fe^{+2}	3.78	2.71	2.73	—	—	0.07	0.23	—
Fe^{+3}	—	—	—	0.01	0.66	—	—	0.88
Mn	0.04	0.04	0.01	—	—	0.01	0.01	0.01
Mg	5.23	6.52	6.74	0.00	0.90	0.00	0.06	0.21
Ca	0.00	0.00	0.01	0.94	1.49	3.94	4.36	4.26
Na	0.02	0.01	0.02	2.66	0.18	0.01	0.00	0.00
K	—	—	—	0.17	0.56	—	—	0.00
Cl	—	—	—	0.87	—	—	—	—
(OH,O)	19.33	18.50	17.97	23.13	33.98	4.23	5.81	6.15

the contact between Sugarloaf diorite and hybrid diorite in the Ajax East pit is metamorphosed to a strongly ...ed, biotite-rich rock. K-feldspar-calcite ± epidote veins, associated with the main stage porphyry alteration, cross-cut the foliation.

Much of the pyroxene in the hybrid diorite unit has been converted to a green-brown hornblende. The occurrence of hornblende-rich pegmatitic and agmatitic phases within this unit, suggests that secondary hornblende in the hybrid diorite may have formed by a late magmatic or deuteric process. Pervasive epidote chlorite assemblages occur in angular interstices between the coarse hornblende and plagioclase laths.

Main Stage Porphyry Alteration

The main alteration stages are divided into propylitic, albitic, potassic and scapolite assemblages. Propylitic and albitic alteration are the dominant assemblages. Propylitic alteration is peripheral to albitic alteration and appears to be a weaker manifestation of the same alteration process. Potassic alteration occurs as irregularly distributed K-feldspar veins cross-cutting pervasive propylitic and albitic alteration zones. Scapolite veins occur only locally in the Ajax East pit, cross-cutting weakly propylitized and albitized rock. A simplified alteration zonation pattern is shown in Figure 8. Representative microprobe analyses (Ross, 1993) of significant minerals are given in Table 2.

Pyrite and chalcopyrite occur on microfractures and as disseminations in propylitized and moderately albitized Sugarloaf diorite and hybrid diorite. Trace amounts of bornite and chalcocite, and minor amounts of molybdenite occur locally. Native copper was observed in oxidized faults in the upper benches of the Ajax West pit. Free gold was not observed in either pit.

The propylitic alteration assemblage is characteristically green due to chlorite and epidote. Most of the chlorite occurs in hybrid diorite, peripheral to both albitic alteration and mineralization. Epidote occurs in veinlets, disseminated in the groundmass, and locally as intense pervasive replacement of host rock. Most epidote is peripheral to intense albitic alteration and copper mineralization.

The mineralogy of propylitic alteration reflects the host rock composition. Propylitized hybrid diorites are veined with barren calcite and epidote veinlets, some with weak albitic envelopes. The intensity of propylitic alteration varies among the phases of hybrid diorite. The only evidence of alteration in fine- to medium-grained diorite is saussuritization of plagioclase and minor overgrowths of Fe-rich prehnite on pyroxene. In the fine-grained, more felsic phase of hybrid diorite that dominates the West pit, propylitic alteration consists of saussuritization of plagioclase and formation of minor amounts of chlorite and epidote. Clear grains of secondary albite (An_{02}) can be distinguished from the cloudy primary plagioclase. Veinlets and pervasive patches of epidote are associated with sparse pyrite and chalcopyrite. Primary magnetite remains unaltered. Pervasive epidote alteration of hybrid diorite occurs locally in the West pit. The coarser grained, pyroxene-rich hybrid diorite in the East pit is intensely chloritized.

Propylitized Sugarloaf diorite contains abundant epidote, disseminated through the groundmass and in veinlets with pyrite and chalcopyrite. Microprobe analyses of epidote in veinlets and in disseminated patches show no clear differences in major element composition. Plagioclase phenocrysts are extensively saussuritized. Secondary feldspars are albite (An_{02}). Hornblende and minor chlorite replace primary hornblende. The groundmass consists of secondary calcite and diopside. Primary magnetite is not affected by propylitic alteration.

Albitic alteration assemblage is characterized by albite, diopside and pyrite. Albitization is best developed in the Sugarloaf diorite at its contacts with hybrid diorite (Fig. 8 C,D). Where albitization is most intense, pyrite is absent and the copper-gold content is low. The higher copper-gold contents are intimately associated with moderate albitization. Pyrite distribution correlates positively with high copper and gold contents. Molybdenite is present in minor amounts and appears to be temporally related to chalcopyrite precipitation.

TABLE 2. (continued)

	Epidote			
Sample	**33 A5 3**	**34 B1 2**	**35 B2 2**	**35 B5 2**
Lithology	**Sugarloaf diorite**	**Sugarloaf diorite**	**hybrid diorite**	**hybrid diorite**
Alteration	**propylitic**	**albitic**	**propylitic**	**propylitic**
SiO_2	36.99	37.48	37.67	36.83
Al_2O_3	21.38	24.40	27.71	23.75
K_2O	—	—	—	—
TiO_2	0.07	0.03	0.04	0.07
FeO	14.10	11.05	6.99	11.25
Fe_2O_3	—	—	—	—
MnO	0.07	0.18	0.26	0.03
MgO	0.01	0.02	0.08	0.01
CaO	23.11	23.03	23.22	23.19
Na_2O	0.01	0.00	0.01	0.00
BaO	—	—	—	—
SrO	—	—	—	—
Cr_2O_3	0.02	0.00	0.00	0.00
NiO	0.00	0.00	0.02	0.00
TOTAL	95.76	96.19	96.00	95.13
FeO/MgO				
Ions based on 8 oxygens				
Si	3.24	3.20	3.15	3.19
Al(IV)	2.20	2.46	2.73	2.43
Ti	0.00	0.00	0.00	0.00
Fe^{+2}	1.03	0.79	0.49	0.82
Mn	0.01	0.01	0.02	0.00
Mg	0.00	0.00	0.01	0.00
Ca	2.17	2.11	2.08	2.15
Na	0.00	0.00	0.00	0.00
Cr	0.00	0.00	0.00	0.00
(OH,O)	13.00	13.00	13.00	13.00

Albitization is first manifested as albitic envelopes around microfractures that typically coalesce to form a massive, dense, white rock composed dominantly of albite with lesser diopside. Primary textures preserved in the less intensely altered rocks, are destroyed at greater intensities, rendering identification of the protolith difficult. Incipient albitic alteration is characterized by: (1) alteration of plagioclase to a cloudy mass, with patches of clear, twinned secondary albite, and (2) replacement of primary hornblende and primary pyroxene by diopside. Albite with chessboard twinning is developed locally. Veinlets of diopside, epidote and albite locally contain sulphides. Secondary pyroxene is diopsidic and slightly more sodic and calcic than the primary pyroxene (Table 2). Pyrite and chalcopyrite occur as disseminations and microveinlets, most often associated with epidote. As the intensity of the alteration increases, titanite with minute inclusions of magnetite replaces diopside. Titanite grains are commonly surrounded by calcite. The albitic assemblage is overprinted by a prehnite-pumpellyite assemblage. Prehnite replaces epidote associated with pyrite and chalcopyrite. Pumpellyite occurs with calcite in cross-cutting veinlets and as replacements of diopside in the groundmass. Prehnite and albite occur in envelopes adjacent to pumpellyite veinlets. It is uncertain if this assemblage represents a retrograde alteration related to waning stages of the porphyry-style mineralization, or if it is a later, regional metamorphic overprint.

The potassic alteration assemblage is marked by K-feldspar that typically occurs as sub-parallel vein swarms within zones of pervasive albitic and propylitic alteration. K-feldspar veins occur in both the hybrid diorite and Sugarloaf diorite units. Secondary biotite replaces pyroxene in the coarse-grained hybrid diorite on the northwestern side of the East pit. The cause of this biotite alteration is not known.

K-feldspar veins are more common in the East pit. They consist of K-feldspar and albite, frequently with calcite, epidote and diopside, but rarely chalcopyrite. The albite in the veins is white and the K-feldspar is salmon pink. Vein selvages consist of chlorite, calcite and actinolite. Vein envelopes are up to 2 cm wide and

TABLE 3. Summary of the common structures for the Ajax West and Ajax East pits

Structure	Vein assemblage	Orientation	Alteration
Ajax West pit			
Faults	Variable: calcite, K-feldspar, quartz, calcite, clay gouge	Variable strike, moderate dip to west	Chlorite and hematite, carbonate
K-feldspar veins	K-feldspar, calcite, pyrite, chalcopyrite	Moderate to steeply northwest dipping	Chlorite
Albite veins	Albite ± epidote ± calcite ± diopside ± pyrite ± chalcopyrite	Variable	Albite, epidote
Quartz veins	Quartz, pyrite	Variable	Hematite, silicification
Ajax East pit			
Faults	Variable: K-feldspar, calcite, quartz, clay gouge	Northeast to northwest, moderately to steeply south dipping	Hematite, chlorite
K-feldspar veins	K-feldspar, albite, epidote, calcite, pyrite, chalcopyrite ± quartz	Dominant northwest strike, minor northeast strike	Chlorite, actinolite, K-feldspar, titanite
Albite veins	Albite ± diopside ± epidote ± calcite ± pyrite ± chalcopyrite	Variable	Albite, epidote, chlorite
Quartz veins	Quartz, K-feldspar, calcite, pyrite	Two sets, northeast strike	Silicification

contain mainly K-feldspar and actinolite. The K-feldspar veins occur singly and in swarms up to several metres across. These veins are neither demonstrably related to the propylitic and albitic alteration that they cut, nor are they well mineralized. K-feldspar, therefore, appears to be relatively late in the main stage mineralization. Microprobe analyses of the potassic veins identifed an albite core (An_{06}) with locally developed chessboard twinning, a K-feldspar (Or_{96}) margin and a middle zone of intermediate feldspar ($Or_{30}Ab_{69}An_{01}$). The chlorites have been identified as ripidolite and pycnochlorite.

A K-feldspar-magnetite-chalcopyrite stockwork/breccia, approximately 5 m long and 2 m wide, occurs on the 960 m bench of the East pit in medium-grained, dark green hybrid diorite. It comprises a subparallel swarm of K-feldspar veins striking 056°, dipping steeply to the southeast and surrounded by magnetite-rich alteration that grades into a breccia of small angular K-feldspar clasts in a magnetite matrix. Chalcopyrite is associated with the magnetite in the breccia. This is an isolated feature and its relationship to the potassic alteration is not clear.

The scapolite alteration assemblage occurs as a stockwork on the 940 m and 960 m benches on the northwestern side of the Ajax East pit, within the hybrid diorite. Individual waxy, grey-green-blue veins are up to 6 cm across. Narrow (3 mm to 5 mm) envelopes of biotite surround the veins and pervasive biotite is developed in a metre wide area in the host rock surrounding the veins. The scapolite occurs as masses of tabular grains in veins with minor interstitial red-brown biotite and chlorite, and rare diopside grains. Red-brown biotite forms a 1 cm wide envelope around the vein, poikiolitically enclosing diopside, which appears to be in equilibrium with the scapolite. The host rock consists of coarse, equant, cloudy relict phenocrysts of pyroxene, minor hornblende, sericitized plagioclase and clear, twinned secondary albite. Microveinlets of calcite and an unidentified mineral, possibly a zeolite, occur perpendicular to and cross-cutting the scapolite veining. A third scapolite occurrence on the 930 m bench is overprinted by a lower temperature assemblage. A pink zeolite similar to heulandite and stilbite (Table 2), partially replaces scapolite, and the biotite envelopes are completely altered to chlorite and actinolite.

Scapolite veins cross-cut disseminated mineralization, but contain minor chalcopyrite. No cross-cutting relationships with intense albitic alteration or with the K-feldspar veining were observed. The scapolite is a chlorine-rich dipyre with a meionite component of 27% (Table 2). There was no evidence of zoning within the grains and no fluid inclusions were observed.

Late Stage Porphyry Alteration

Deuteric epidote and potassic alteration is associated with the late- to post mineral monzodiorite dikes. Epidote is often disseminated throughout the groundmass of these dikes and is a common coating on joint surfaces. K-feldspar alteration is pervasive in some dikes, but absent in others.

Post Porphyry Alteration

Quartz veins are related spatially to post-porphyry quartz eye latite dikes. Veins are vuggy, with buff coloured silicification envelopes that are less than 0.5 m wide. Pyrite-bearing, vuggy, epithermal quartz veins, surrounded by silicic envelopes, were observed in the West pit. These veins are probably genetically related to the quartz eye latite dikes.

Regionally the rocks are characterized by low-grade, greenschist facies alteration (Carr and Reed, 1976). Pumpellyite, prehnite and zeolites are common in both the batholith (Carr, 1956) and the Nicola Group volcanic rocks (Preto, 1979) and may be related to burial metamorphic effects.

Structure

The rocks within both the West and East pits are intensely fractured and faulted. Although minor (1 m to 3 m) offsets were observed on some faults, the lack of marker units precludes more detailed determination of offset direction or magnitude. Faulted contacts between several of the units form the major structural features within the pits. In the West pit, the faulted east-west trending contact between hybrid diorite and Sugarloaf diorite divides the pit into two domains. The East pit is divided into two domains along a northeasterly trending contact between these same two units. These major faults are near the foci of mineralization and alteration in both pits. They do not substantially offset either mineralized zones or alteration.

There are several stages of irregular and widely-spaced veins (1 vein per 2 m). Although cross-cutting relationships are not definitively constrained, a general paragenetic sequence has been established. Veins have been divided into: (1) albite-epidote-calcite ± sulphide veins with albitic envelopes; (2) K-feldspar-calcite ± epidote ± albite ± sulphide veins with chlorite-actinolite envelopes; (3) quartz veins; and (4) calcite veins. The albite-bearing veins are wispy and discontinuous, and are seldom more than 1 m to 2 m long. The K-feldspar veins are more abundant and continuous in the East pit, where they occur in swarms. Quartz veins, which occur in both pits, are planar and continuous. There are two types of quartz veins: (1) purplish quartz veins with hematitic envelopes, and (2) vuggy epithermal quartz-pyrite veins with silicic envelopes (related to the quartz eye latite dikes). The purple-quartz veins occupy faults, whereas the quartz-pyrite veins cross-cut most faults. Calcite veins appear to have formed during at least two stages. Massive calcite-chalcopyrite veins related to main stage mineralization occur local-

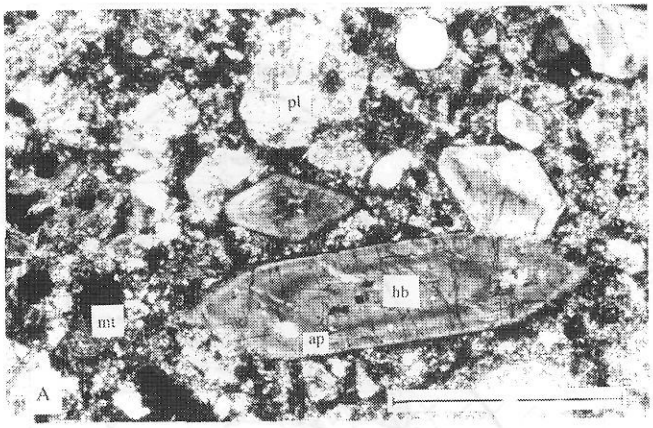

FIGURE 8A. Thin section of typical Sugarloaf diorite exhibiting euhdral, zoned hornblendes and tabular plagioclase with accessory magnetite and apatite. Abbreviations: ap = apatite, mt = magnetite, pl = plagioclase, hb = hornblende. (Scale bar 1 mm)

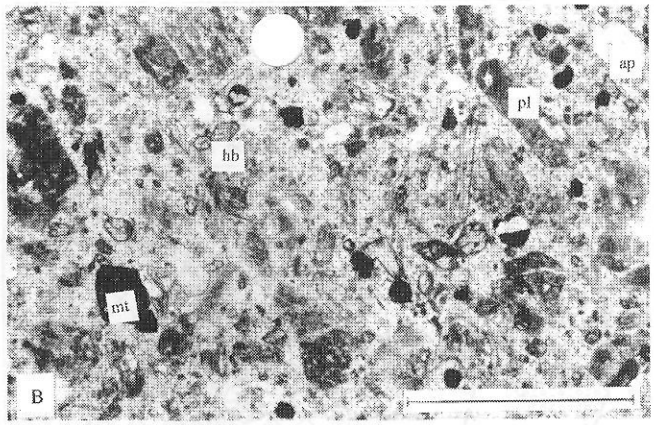

FIGURE 8B. Thin section of a monzonite dike. These dikes are both texturally and compositionally similar to the Sugarloaf diorite and may be a late phase of this unit. Abbreviations: ap = apatite, mt = magnetite, pl = plagioclase, hb = hornblende. (Scale bar 1 mm.)

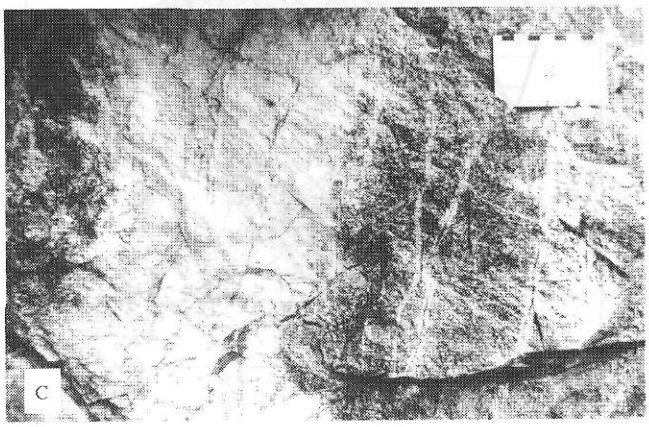

FIGURE 8C. Hand sample of albitic alteration. Albitic alteration occurs as envelopes about sulphide veinlets and coalesces to form a massive white rock.

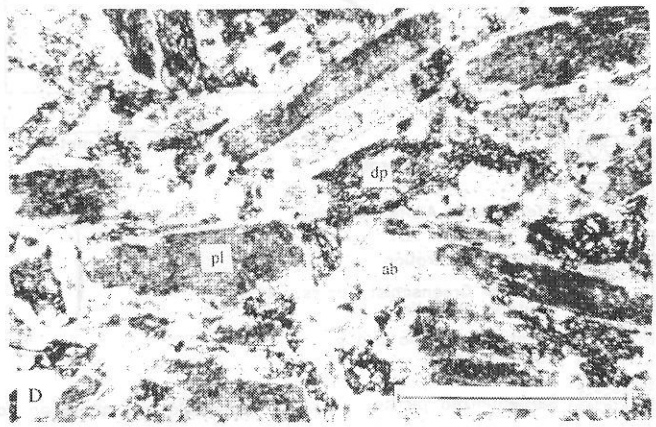

FIGURE 8D. Thin section of moderate albitic alteration in Sugarloaf diorite. Phenocrysts are still recognizable but primary plagioclase is converted to cloudy secondary albite and hornblende is largely converted to diopside. Abbreviations: ab = albite, pl = plagioclase, dp = diopside. (Scale bar 1 mm)

ly in both pits, but most calcite appears to be predominantly post-mineral. Unmineralized calcite stockworks occur in both pits.

Several sulphide-carbonate breccias occur in the West pit. They are less than 1 m wide and range from 1 m to 5 m in length. A larger sulphide breccia body (5 m by 5 m) along the contact between hybrid diorite and Sugarloaf diorite was exposed during mining of the 830 m bench in the West pit. This breccia consisted of a matrix of fine-grained pyrite-chalcopyrite-calcite cementing angular fragments of albitized Sugarloaf diorite (Bond, 1991).

The structural domain in the southern half of the West pit is underlain by Sugarloaf diorite. Intensely albitized rock forms resistant blocks around which more chloritic rocks have developed a weak foliation. The northern half of the pit is underlain by chloritized, hematized and faulted hybrid diorite. Barren calcite veins are developed on faults. The structural data for both domains (Table 3) have been subdivided into faults and veins. Most faults in both domains strike northeast to northwest, dip to the west, and are unmineralized. K-feldspar-chalcopyrite and albite ± epidote ± calcite veins generally dip to the northwest.

The northwestern structural domain of the East pit is underlain by hybrid diorite. The northern section is intensely faulted, hematized and chloritized, but the southern section lies outside the area affected by intense alteration and mineralization. Fault orientations vary, but both barren and chalcopyrite-bearing faults dip south. K-feldspar veins strike dominantly northwest and albite veins have no preferred orientation. Quartz veins occur in two distinct sets, one northwest trending and the other northeast trending. The southeastern half of the pit is underlain by albitic and propylitic, altered Sugarloaf diorite, characterized by blocks of resistant, albitized Sugarloaf diorite surrounded by propylitized, weakly foliated diorite. Faults strike northwest and northeast with steep southwestly dips. Most chalcopyrite-bearing faults strike to the northwest. K-feldspar veins strike northwest and dip northeast and southwest. The orientation of albite veins varies widely.

The Iron Mask batholith lies along a regional northwesterly trending structure (Carr and Reed, 1976). Northwest and west trending linear structures cut the pluton and serve as the locus for younger intrusive phases, such as the Sugarloaf diorite. The orientation of the K-feldspar veins reflects this regional trend, whereas the albite veins do not. Structural orientations differ between the West and East pits. In the West pit chalcopyrite-bearing K-feldspar and albite veins strike northeast and dip northwest. In the East pit chalcopyrite-bearing veins strike northwesterly and northeasterly, but both have dips from south to vertical. The difference in structural orientations may be controlled by the orientation of the major fault contacts. The main fault in the West pit strikes east-west, whereas in the East pit the main faulted contact strikes northeast.

Unmineralized faults in both orebodies are concordant with the dominant southeast to east-southeast strike of regional faults and represent a late Mesozoic to Early Tertiary structural overprint on earlier structures.

Discussion and Conclusions

The simplified deposit model of Figure 9 illustrates the altera-

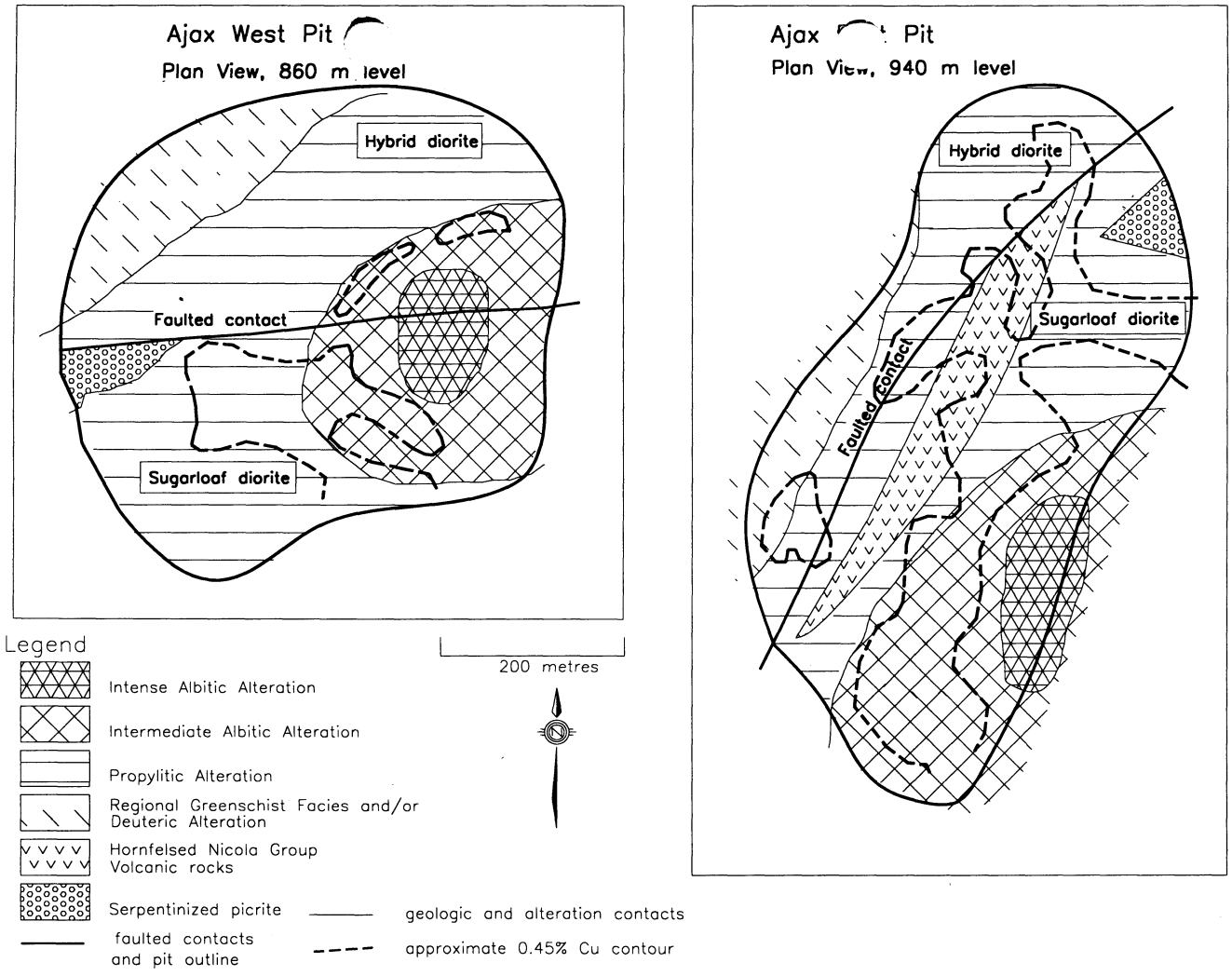

FIGURE 9. Schematic deposit scale alteration model of the Ajax deposits. A core of intense albitic alteration is surrounded by intermediate intensity albitic alteration, grading out into propylitic alteration and finally into the regional greenschist facies and deuteric alteration. Potassic and scapolitic alteration occurs locally as veins, cross-cutting both albitic and propylitic alteration. Intense albitization is developed predominantly in the Sugarloaf diorite. Copper-gold mineralization occurs in albitic and propylitic alteration zones, but the highest grades occur in the intermediate intensity albitic alteration. The 0.45% Cu grade contour, determined from blasthole data on the 860 metre level in the Ajax West pit and the 940 metre level in the Ajax East pit, is shown.

tion zoning in the Ajax East and Ajax West deposits. Sugarloaf diorite was intruded into the hybrid diorite along regional east-west and northeast trending fault structures. Alteration and copper-gold mineralization is focussed along the contact between the hybrid diorite and Sugarloaf diorite. Alteration assemblages formed as partial shells around the Sugarloaf intrusion, but the strong lithologic controls on alteration prevented the formation of true concentric shells. A diffuse core of intense albitic alteration with low-grade (0.11% Cu, 0.1 g/t Au) copper-gold mineralization, surrounded by intermediate intensity albitization with high-grade (0.64% Cu, 0.40 g/t Au) copper-gold mineralization is concentrated on the Sugarloaf diorite. Peripheral to this zone is a zone of propylitic alteration with low to moderate grades (0.14% to 0.35% Cu, 0.08 g/t to 0.22 g/t Au) of copper-gold mineralization, which grades outward into a regional greenschist facies metamorphism. Fracture controlled K-feldspar veins carrying minor chalcopyrite-pyrite cross-cut albitic and propylitic alteration. Scapolite veins, also with minor chalcopyrite, cross-cut propylitic alteration.

The association of albitic alteration with copper-gold mineralization and the occurrence of a later fracture-controlled potassic alteration are two characteristic features of the Ajax deposits. These characteristics have been observed at other alkaline copper-gold porphyry deposits (Table 4). Within the Iron Mask batholith, the Pothook, Big Onion, Ajax and probably the Afton deposits occur along contacts between Pothook (hybrid) diorite and Nicola Group volcanic rocks which have been intruded by Sugarloaf diorite. Alteration style is characterized by an early mineralized, pervasive albitic alteration, cross-cut by fracture-controlled K-feldspar alteration with minor chalcopyrite and pyrite. In addition, the Pothook deposit is overprinted by gold-copper mineralizing chlorite-magnetite-hematite veins (Lang and Stanley, this volume). The Crescent and DM deposits occur at the contact of Pothook diorite and Cherry Creek monzonite. These deposits are characterized by unmineralized, pervasive K-feldspar alteration related to intrusion of the Cherry Creek monzonite, cross-cut by fracture-controlled, chalcopyrite-bearing K-feldspar-chlorite-magnetite veins. Later quartz-calcite veins and breccias host minor copper-gold mineralization (Lang and Stanley, this volume). Similar styles of mineralization and alteration have been recognized in other alkalic porphyry deposits. At Copper Mountian and Ingerbelle (Preto, 1972; Fahrni et al., 1976), mineralized, pervasive albitic alteration has been overprinted by late stage fracture controlled K-feldspar veins. At Copper Mountain the K-feldspar veins carry minor chalcopyrite and bornite. Unmineralized late stage scapolite veins are common at Ingerbelle. At Mt. Milligan (DeLong and Godwin, 1991) potassic alteration is widespread, but locally intense albitic alteration is associated with good ore grades. At Mount Polley (Fraser, 1994), sulphides are hosted in a hydrothermal albite breccia and albite veins

TABLE 4. Summary of characteristics of the signficant ore deposits hosted in the Iron Mask pluton

Deposit	Size (tonnes)	Production/ Reserves	% Cu	g/t Au	Intrusive host rock	Alteration	Mineralization control	References
Afton (Open Pit) Underground	22 136 000 9 525 000	Past Production Geologic Reserves	0.91 1.50	0.67 1.10	hybrid diorite? Cherry Creek monzonite?	pervasive propylitic-magnetite sporadic potassic supergene enrichment	supergene alteration of propylitic-magnetite assemblage	Carr and Reed, 1976 Kwong, 1987
Ajax West	18 325 000	Pre-Mining Reserves	0.47	0.37	Sugarloaf diorite hybrid diorite	pervasive albitic-propylitic, late stage K-feldspar	pervasive albitization	Ross et al., 1992 Ross, 1993
Ajax East	6 350 000	Pre-Mining Reserves	0.44	0.37	Sugarloaf diorite hybrid diorite	pervasive albitic-propylitic, late stage K-feldspar and scapolite	pervasive albitization	Ross et al., 1993 Ross, 1993
Pothook	2 359 000	Past Production	0.35	0.77	Pothook diorite Cherry Creek monzonite Sugarloaf diorite	pervasive potassic related to Cherry Creek, pervasive albitic related to Sugarloaf, late cross-cutting K-feldspar-biotite-epidote veins, Fe-oxide-Cu-sulphide veins	late fracture controlled Fe-oxide-Cu-sulphide veins	Stanley, 1994
Crescent	1 448 000	Past Production	0.44	0.17	Pothook diorite Cherry Creek monzonite	pervasive potassic related to Cherry Creek late magnetite, K-feldspar, chlorite-magnetite, epidiote, calcite-quartz veins hydrothermal breccias	chlorite-magnetite-sulphide veins and some in open space breccias	Lang, 1994
DM	2 685 000	Reserves	0.38	0.27	Pothook diorite Cherry Creek Sugarloaf diorite	pervasive potassic within intrusion breccias later magnetite, K-feldspar, chlorite-magnetite, epdiote, calcite-quartz veins	chlorite-magnetite and quartz dominant veins hosted in intrusion breccias	Lang and Stanley, this volume
Big Onion	3 266 000	Reserves	0.71	0.44	Sugarloaf diorite Picrite	pervasive albitic, K-feldspar-biotite-magnetite-sulphide veins	albitic alteration and K-feldspar veins, timing unclear	Lang, pers. comm., 1994

cross-cut actinolite veins with K-feldspar envelopes. Sulphide-bearing magnetite-K-feldspar breccias are also locally developed (Fraser, 1994), similar to K-feldspar-magnetite-chalcopyrite breccia seen in the Ajax East pit. In conclusion, an early, intense Na-metasomatic stage appears to be a common feature in many alkaline porphyry systems, with frequent later development of fracture-controlled potassic alteration and occassionally even later development of scapolite veins.

In all the Iron Mask deposits, albitic alteration is intimately associated with the intrusion of the Sugarloaf diorite. The spatial relationship of Sugarloaf diorite to albitic alteration and copper-gold mineralization suggests that it is the main mineralizing intrusion. Disseminated chalcopyrite, generally associated with pyrite and lesser secondary magnetite, is present in many exposures of Sugarloaf diorite throughout the Iron Mask batholith (Stanley et al., 1994). The Na-rich nature of the alteration is probably a direct consequence of the relatively Na-rich nature of fresh Sugarloaf diorite (Fig. 6). A fluid exsolved from this dioritic magma would also be sodic. The conversion of plagioclase- and hornblende-bearing Sugarloaf diorite to massive albite and diopside consumes Na^+, H^+ and SiO_2, and releases Fe^{2+}, Ca^{2+} and H_2O. The consumption of silica by the reaction may partly explain the absence of quartz veins in the system. The liberated Fe^{2+} is available to react with Cu and S in solution to precipitate chalcopyrite according to the reaction:

$$Fe^{2+} + CuCl^{o}(aq) + 2H_2S(aq) = CuFeS_2 + Cl^{-}(aq) + 4H^{+}(aq)$$

The H^+ released in this reaction lowers the pH which in turn may increase albitization, releasing more Fe^{2+}, resulting in further chalcopyrite precipitation. Ca^{2+} reacts with CO_3 to form calcite and with Fe^{2+} and Al^- to form epidote, both intimately associated with chalcopyrite and pyrite precipitation. The propyltic assemblage represents a weaker manifestation of the albitizing process. Fluids flowing from cooler country rock into the higher temperature intrusive would exchange K^+ in the rock for Na^+ in solution (Carten, 1986), possibly providing the K^+ for the late K-feldspar veins. The presence of late Cl-rich scapolite veins indicates the evolution of a volatile rich fluid.

The common association of picrite, Sugarloaf diorite and mineralization may reflect similar controls by regional fault structures. Foliated, biotitized Nicola Group volcanic rocks and serpentinized picrite occur along the faulted contact between hybrid diorite and Sugarloaf diorite in both the Ajax East and Ajax West pits. Picrite also occurs in close proximity to the Afton (Carr and Reed, 1976; Kwong, 1987), Big Onion (Preto, 1967), Galaxy and Python (Carr, 1956) deposits. Picrite does not play an active role in mineralization, but does denote the presence of major faults.

Several conclusions may help in future mineral exploration in the Iron Mask batholith. The Sugarloaf diorite appears to be the mineralizing unit, so its occurrence is of paramount importance. Mineralization is concentrated at the contact of this unit with the hybrid diorite. The distinction between propylitic alteration associated with a productive porphyry and regional greenschist alteration is not obvious, but the frequent presence of disseminated pyrite and a more intense albitization of plagioclase phenocrysts in the propylitic assemblage may be used as a guide. Intense albitization with low grade copper-gold mineralization may be spatially related to intermediate albitization with higher grade mineralization. Although generally poorly mineralized, K-feldspar veins are part of the porphyry mineralizing event and are potential indicators of mineralization. Strong foliation and biotitization of Nicola Group volcanic rocks are guides to mineralization by analogy to the remnant in the Ajax East pit. Intensely serpentinized picrite follows major faults that may also focus the intrusion of the young Sugarloaf diorite intrusions. The majority of deposits and prospects within the batholith are located near the margins of the batholith and many, if not all, are related to major faults.

Acknowledgments

This study formed part of the requirements for an M.Sc. degree at The University of British Columbia. Research was supported by the Geological Survey of Canada and the Mineral Deposit Research Unit at the Department of Geological Sciences, The University of British Columbia, through the Collaborative Industry SCBC-NSERC research project, "Copper-gold Porphyry Deposits of British Columbia". Financial support from a COSEP Grant to Ross is gratefully acknowledged. Afton Operating Corporation provided access to company files, drill core and the mine property. Wayne Spilsbury, of Teck Corporation, helped focus the project. This paper benefitted from critical reviews by J.R. Lang, R.V. Kirkham and C.W. Jefferson.

REFERENCES

BOND, L., 1991. Geology and development of the Ajax copper-gold deposits. Unpublished company report, Afton Mining Corporation.

CARR, J.M., 1956. Deposits associated with the eastern part of the Iron Mask batholith near Kamloops. British Columbia Department of Mines Annual Report 1956, p. 47-69.

CARR, J.M. and REED, A.J., 1976. Afton: A supergene copper deposit. *In* Porphyry Deposits of the Canadian Cordillera. *Edited by* A. Sutherland Brown. Canadian Institute of Mining and Metallurgy, Special Volume 15, p. 376-387.

CARTEN, R.B., 1986. Sodium-calcium metasomatism: Chemical, temporal, and spatial relations at the Yerington, Nevada, porphyry copper deposit. Economic Geology, 81, p. 1495-1519.

COCKFIELD, W. E., 1948. Geology and mineral deposits of Nicola map area, British Columbia. Geological Survey of Canada, Memoir 249.

DELONG, R.C. and GODWIN, C.I., 1991. Geology and alteration at the Mt. Milligan gold-copper porphyry deposit, Central British Columbia (93N/1E). *In* Geological Fieldwork 1990. British Columbia Ministry of Energy, Mines and Petroleum Resources, Paper 1991-1, p. 199-205.

FAHRNI, K.C., MACAULEY, T.N. and PRETO, V.A., 1975. Copper Mountain and Ingerbelle. *In* Porphyry Deposits of the Canadian Cordillera. *Edited by* A. Sutherland Brown. Canadian Institute of Mining and Metallurgy, Special Volume 15, p. 368-375.

FRASER, T., 1994. Hydrothermal breccias and associated alteration of the Mount Polley copper-gold deposit. *In* Geological Fieldwork 1993. British Columbia Ministry of Energy, Mines and Petroleum Resources, Paper 1994-1, p. 259-267.

IRVINE, T.N. and BARAGAR, W.R.A., 1971. A guide to the chemical classification of the common volcanic rocks. Canadian Journal of Earth Sciences, 8, p. 523-548.

KWONG, Y.T.J., 1987. Evolution of the Iron Mask batholith and its associated copper mineralization. British Columbia Ministry of Energy, Mines and Petroleum Resources, Bulletin 77, p. 1-55.

LANG, J.R. 1994. Geology of the Cresent alkalic porphyry copper-gold deposit, Afton Mining Camp. British Columbia (92I/9,10). *In* Geological Fieldwork 1993. British Columbia Ministry of Energy, Mines and Petroleum Resources, Paper 1994-1, p. 285-293.

LANG, J.R. and STANLEY, C.R., 1995. Contrasting styles of alkalic porphyry copper-gold deposits in the northern part of the Iron Mask batholith, Kamloops, British Columbia. *In* Porphyry Deposits of the Northwestern Cordillera of North America. *Edited by* T.G. Schroeter. Canadian Institute of Mining, Metallurgy and Petroleum, Special Volume 46.

LANG, J.R., STANLEY, C.R. and THOMPSON, J.F.H., 1992. Quartz alkalic and nepheline alkalic: Two distinct subtypes of porphyry deposits related to alkalic igneous rocks. Geological Society of America, Program with Abstracts, Volume 24, p. A143.

MIDDLEMOST, E.A.K., 1975. The Basalt Clan. Earth Science Review, 11 (4), p. 337-364.

MONGER, J.W.H., WHEELER, J.O., TIPPER, H.W., GABRIELSE, H., HARMS, T., STRUIK, L.C., CAMPBELL, R.B., DODDS, C.J., GEHRELS, G.E. and O'BRIEN, J., 1991. Part B. Cordilleran Terranes. *In* Chapter 8 Upper Devonian to Middle Jurassic Assemblages, The Geology of the Cordilleran Orogen in Canada. Geological Survey of Canada, No. 4, p. 281-327 (also, Geological Society of America, The Geology of North Americal, V. G-2).

MORTENSEN, J.K., GOSH, D. and FERRI, F., 1995. U-Pb geochronometry of intrusive rocks associated with copper-gold deposits in the Canadian Cordillera. *In* Porphyry Deposits of the Northwestern Cordillera of North America. *Edited by* T.G. Schroeter. Canadian Institute of Mining, Metallurgy and Petroleum, Special Volume 46.

NORTHCOTE, K.E., 1974. Geology of the northwest half of the Iron Mask batholith. *In* Geological Fieldwork, 1974, Paper 1975-1. British Columbia Department of Mines and Petroleum Resources, p. 22-26.

NORTHCOTE, K.E., 1976. Geology of the southeast half of the Iron Mask batholith. *In* Geological Fieldwork, 1976, Paper 77-1. British Columbia Department of Mines and Petroleum Resources, p. 41-46.

NORTHCOTE, K.E., 1977. Geological map of the Iron Mask batholith and accompanying notes. British Columbia Ministry of Energy, Mines and Petroleum Resources, 8 p.

PRETO, V.A., 1967. Geology of the eastern part of the Iron Mask batholith. British Columbia Ministry of Mines and Petroleum Resources, Annual Report 1967, p. 137-147.

PRETO, V.A., 1972. Geology of Copper Mountain. British Columbia Department of Mines and Petroleum Resources, Bulletin 59, 87 p.

PRETO, V.A., 1977. The Nicola Group: Mesozoic volcanism related to rifting in southern British Columbia. *In* Volcanic Regimes in Canada. *Edited by* W.R.A. Baragar, L.C. Coleman and J.M. Hall. Geological Association of Canada, Special Paper No. 16, p. 39-57.

PRETO, V.A., 1979. Geology of the Nicola Group between Merritt and Princeton. British Columbia Ministry of Energy, Mines and Petroleum Resources, Bulletin 69, 90 p.

PRETO, V.A., OSATENKO, M.J., McMILLAN, W.J. and ARMSTRONG, R.L., 1979. Isotopic dates and strontium isotopic ratios for plutonic and volcanic rocks in the Quesnel Trough and Nicola Belt, south-central British Columbia. Canadian Journal of Earth Sciences, 16, p. 1658-1672.

ROSS, K.V., 1993. Geology of the Ajax East and Ajax West, silica-saturated alkalic copper-gold porphyry deposits, Kamloops, south-central, British Columbia. Unpublished M.Sc. thesis. The University of British Columbia, Vancouver, British Columbia, 210 p.

ROSS, K.V., DAWSON, K.M., GODWIN, C.I. and BOND, L., 1992. Major lithologies of the Ajax West pit, an alkalic copper-gold porphyry deposit, Kamloops, British Columbia. *In* Current Research, Part A. Geological Survey of Canada, Paper 92-1A, p. 179-183.

ROSS, K.V., DAWSON, K.M., GODWIN, C.I. and BOND L., 1993. Lithologies and alteration of the Ajax East zone, an alkalic copper-gold porphyry deposit, Kamloops, British Columbia. *In* Current Research, Part A. Geological Survey of Canada, Paper 93-1A, p. 87-95.

SNYDER, L.D. and RUSSELL, J.K., 1993. Field constraints on diverse igneous processes in the Iron Mask batholith (92I/9,10). *In* Geological Fieldwork 1992. British Columbia Ministry of Energy, Mines and Petroleum Resources, Paper 1993-1, p. 269-274.

SNYDER, L.D. and RUSSELL, J.K., 1995. Petrogenetic relationships and assimilation processes in the alkalic Iron Mask batholith, south-central British Columbia. *In* Porphyry Deposits of the Northwestern Cordillera of North America. *Edited by* T.G. Schroeter. Canadian Institute of Mining, Metallurgy and Petroleum, Special Volume 46.

SOUTHER, J.G., 1992. Volcanic regimes. *In* Chapter 14, Geology of the Cordilleran Orogen in Canada. *Edited by* H. Gabrielse and C.J. Yorath. Geological Survey of Canada. Decade of North American Geology Project, Paper No. 4, p. 457-490.

STANLEY, C.R., 1994. Geology of the Pothook alkalic porphyry copper-gold deposit, Afton Mining Camp, British Columbia (92I/9,10). *In* Geological Fieldwork 1993. British Columbia Ministry of Energy, Mines and Petroleum Resources, Paper 1994-1, p. 275-284.

STANLEY, C.R. and LANG, J.R., 1993. Geology, geochemistry, hydrothermal alteration and mineralization in the Virginia Zone, Copper Mountain copper-gold camp, Princeton, British Columbia. *In* Geological Fieldwork 1992, Paper 1993-1. British Columbia Ministry of Energy, Mines and Petroleum Resources, p. 259-268.

STANLEY, C.R., LANG, J.R. and SNYDER, L.D., 1994. Geology and mineralization in the northern part of the Iron Mask pluton, Iron Mask batholith, British Columbia, (92I/9,10). *In* Geological Fieldwork 1993, Paper 1994-1. British Columbia. Ministry of Energy, Mines and Petroleum Resources, p. 41-46.

WOODSWORTH, G.J., ANDERSON, R.G. and ARMSTRONG, R.L., 1992. *In* Chapter 15, Plutonic Regimes. *In* Geology of the Cordilleran Orogen in Canada. *Edited by* H. Gabrielse and C.J. Yorath. (Also, Geological Society of America, The Geology of North America, V. G-2).